

Master of Sciences in Bioengineering

***Carbon nanotubes as a novel platform for
L-asparaginase immobilization***

Master's Thesis

by

João Gonçalves Pinho

Dissertation for Master degree in Biological Engineering

Performed at

Associate Laboratory LSRE-LCM,

Department of Chemical Engineering

Faculdade de Engenharia, Universidade do Porto



**Supervisors: Dr. Raquel O. Cristóvão,
Dr. Cláudia G. Silva and
Dr. Ana Paula M. Tavares**

June, 2020

Acknowledgements

First, I want to thank my supervisors, Dr. Raquel Cristóvão, Dr. Cláudia Silva and Dr. Ana Paula Tavares for the opportunity and the availability, interest, motivation, support and competence guiding me in this work. Their knowledge and experience had a very important role in the development of this work.

I also have to thank Eng. Maria Amélia Barros for the carbon nanotubes characterization and João Nunes for the guidance in the determination of Isoelectric point of L-asparaginase.

Then, I want to thank my parents, siblings and grandparents that always showed me an unconditional love and support throughout my life and academic journey and had to put up with me during this pandemic times. Without them, this project would not be possible.

Lastly, I have to thank my friends, especially, Pedro Costa and Telmo Vieira, which whom I had the pleasure to share all my university years and I wouldn't be able to reach my last year this fast without our mutual work, and my friends Inês Ribas, André Silva and Afonso Lei, for all the emotional support during the years, particularly in the last few months.

There was no way that this work could be done without the help and support from these persons.

This work was financially supported by Base Funding - UIDB/50020/2020 of the Associate Laboratory LSRE-LCM - funded by national funds through FCT/MCTES (PIDDAC). This master thesis was developed within the project POCI-01-0145-FEDER-031268 - funded by FEDER, through COMPETE2020 - Programa Operacional Competitividade e Internacionalização (POCI), and by national funds (OE), through FCT/MCTES.

Resumo

A L-asparaginase (L-ASNase) é uma enzima que tem vindo a provar a sua importância comercial ao longo dos anos. Atualmente, a L-ASNase é utilizada na indústria alimentar para inibir a formação de acrilamida, uma substância produzida em alimentos fritos e potencialmente carcinogénica. Na indústria farmacêutica, esta enzima é utilizada como um biofármaco no tratamento da leucemia linfoblástica aguda (ALL), o tipo de cancro mais comum nas crianças. A imobilização desta enzima apresenta vantagens, tanto de interesse para a indústria alimentar, onde poderá ser recuperada e reutilizada mais facilmente, além de aumentar a sua estabilidade e tempo de vida, como para a indústria farmacêutica, onde o suporte de imobilização pode diminuir a afinidade da L-ASNase com os antigénios do organismo, reduzindo assim os efeitos alérgicos. Os nanotubos de carbono (CNTs) são um suporte promissor para a imobilização da L-ASNase, devido à sua elevada área superficial, estrutura hidrofóbica e bioafinidade. Além disso, podem ser funcionalizados, de modo a aumentar a sua afinidade com as enzimas e reduzir a sua eventual toxicidade. Contudo, há várias optimizações necessárias para se obter uma imobilização eficiente.

Neste trabalho de tese foi otimizado o pH e o tempo de imobilização da adsorção física da L-ASNase em CNTs com diferentes diâmetros, não modificados ou funcionalizados com grupos essencialmente do tipo ácido carboxílico através da sua oxidação hidrotérmica com HNO₃. Os resultados foram discutidos tendo em consideração a área superficial dos CNTs e o ponto isoelétrico desta enzima.

Tanto a L-ASNase livre como a imobilizada apresentaram maior atividade a pH 8, o que levou a confirmar que, dado o ponto isolétrico da enzima e o ponto de carga zero dos CNTs, as interações electroestáticas não são as interações mais importantes na adsorção desta enzima neste suporte, sendo as hidrofóbicas e pontes de hidrogénio, provavelmente as interações principais. Após imobilização da enzima nos CNTs funcionalizados com diâmetros de 10 a 20 nm a pH 8 durante 30 minutos, atingiu-se uma atividade recuperada relativa da enzima de cerca de 88±7%, com um rendimento de imobilização de cerca de 96%. É de notar que, devido às suas maiores áreas superficiais específicas e menor hidrofobicidade, os CNTs funcionalizados apresentaram maiores atividades recuperadas relativas da enzima. Estes resultados mostram que os CNTs funcionalizados são suportes promissores para a imobilização de L-ASNase, necessitando de baixos tempos de imobilização para obter bons resultados.

Palavras-chave: L-asparaginase; Imobilização de enzimas; Nanotubos de carbono; Leucemia linfoblástica aguda; Mitigação da acrilamida.

Abstract

L-asparaginase (L-ASNase) is an enzyme that has been proving its commercial value over the years. Currently, L-ASNase is used in the food industry to inhibit acrylamide formation, a potentially carcinogenic substance, produced in fried foods. In the pharmaceutical industry it is used as a biopharmaceutical in the treatment of acute lymphoblastic leukemia (ALL), the most common type of cancer in children. The immobilization of this enzyme has advantages for both food industry, where it can be easily recovered and reused, in addition to enhanced the enzyme stability and half-life, as well as for pharmaceutical industry, where the immobilization support can decrease L-ASNase affinity with antigens, thus reducing the allergic effects to which this enzyme is associated. Carbon nanotubes (CNTs) are a promising support for L-ASNase immobilization due to its high surface area, hydrophobic structure and bioaffinity. In addition, they can be easily functionalized, increasing their affinity with enzymes and reducing their possible toxicity. However, optimal conditions are still needed to be studied in order to achieve an efficient immobilization.

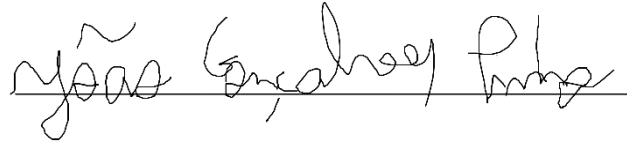
In this thesis, the immobilization parameters, pH and immobilization time, of L-ASNase physical adsorption onto different diameter pristine or functionalized CNTs with essentially carboxylic acid groups through hydrothermal oxidation treatment with NHO_3 , were optimized. The results were discussed taking into account the CNTs surface area and the isoelectric point of this enzyme.

Both free and immobilized L-ASNase showed higher activity at pH 8, which led to confirm, that, given the enzyme isoelectric point and the point of zero charge of the CNTs, electrostatic interactions are not the most important forces involved in the enzyme adsorption on this support, being hydrophobic and hydrogen bonds the probable main driving forces. After 30 min immobilization onto functionalized CNTs with diameters from 10 to 20 nm at pH 8, a L-ASNase relative recovered activity of about $88 \pm 7\%$ and an immobilization yield of 96% were attained. It should be noted that, due to their larger specific surface areas and less hydrophobicity, functionalized CNTs showed higher enzyme relative recovered activities. These results show that functionalized CNTs are promising supports for L-ASNase immobilization, requiring short immobilization times in order to obtain good results.

Keywords: L-asparaginase; Enzyme immobilization; Carbon nanotubes; Acute lymphoblast leukemia; Acrylamide mitigation

Declaration

It is declared on oath that this work is original and that all non-original contributions have been properly referenced with the identification of the source.

A handwritten signature in black ink, reading "João Gonçalves Pinho", written over a horizontal line.

(João Gonçalves Pinho)

List of contents

List of contents	i
List of Figures	iii
List of Tables	iv
Glossary	v
1 Introduction	1
1.1 Project background	1
1.2 Contributions of this work and main goals	2
1.3 Thesis Organization	2
2 Literature review and state-of-the-art.....	4
2.1 L-ASNase - mechanism, structure and sources	4
2.2 L-ASNase in food industry.....	7
2.3 L-ASNase in therapeutic sector	8
2.3.1 L-ASNase as chemotherapeutic agent	8
2.3.2 Side effects of L-ASNase as a therapeutic drug	11
2.4 Enzymes immobilization	12
2.5 Carbon nanotubes	17
2.5.1 Immobilization of biomolecules on CNTs.....	18
2.5.2 CNTs toxicity	19
3 Materials and methods	21
3.1 Materials	21
3.2 Methods	21
3.2.1 General solutions	21
3.2.2 MWCNTs functionalization.....	22
3.2.3 Characterization of CNTs.....	22
3.2.4 Determination of isoelectric point	22
3.2.5 L-ASNase activity measurement	22
3.2.6 Optimization of L-ASNase immobilization.....	24

4	Results and discussion	25
4.1	Characterization of carbon nanotubes	25
4.2	Determination of L-ASNase isoelectric point.....	27
4.3	Effect of pH on L-ASNase onto CNTs	28
4.4	Effect of immobilization time on L-ASNase immobilization onto CNTs ..	32
5	Conclusions	35
6	Future work	36
7	Final appreciation	37
8	Bibliography	38
	Appendix 1 - Calibration curve for ammonia quantification	1

List of Figures

Figure 1 - L-asparaginase reaction mechanism.	4
Figure 2 - L-Asp (left) and L-Gln (right) structures.....	5
Figure 3 - Crystal structure of E. coli L-ASNase I (left) and L-ASNase II (right).	6
Figure 4 - Generic amino acid pathway and different paths to acrylamide production from L-asparagine.....	7
Figure 5 - Schematic example of L-ASNase effect on ALL- A - Normal blood vessel; B - Blood vessel overwhelmed with Lymphocytes; C - Blood vessel from B, after treatment with L-ASNase.	9
Figure 6 - Different matrices used for enzyme immobilization.....	13
Figure 7 - Schematic representation of different enzyme immobilization methods. .	14
Figure 8 -Structure of (A) SWCNTs and (B) MWCNTs.	17
Figure 9 - CNTs after centrifugation: A - CNT <10; B - f-CNT <10; C - CNT 10-20; D - f-CNT 10-20; E - CNT 20-40; F - f- CNT 20-40; G - CNT 60-100; H - f-CNT 60-100	26
Figure 10 - L-ASNase potential zeta values for different pH values.....	28
Figure 11 - Effect of pH on the relative recovered activity in the immobilization of 0.086 mg/mL of L-ASNase onto 2 mg of CNTs for 60 min of contact time.	29
Figure 12 - Effect of pH on the immobilization yield (%) of L-ASNase (0.086 mg/mL) immobilization onto 2 mg of CNTs for 60 min of contact time.	31
Figure 13 - Effect of immobilization time on the relative recovered activity in the immobilization of 0.086 mg/mL of L-ASNase onto 2 mg of CNTs at pH 8	33
Figure 14 -Effect of immobilization time on the relative recovered activity in the immobilization of 0.086 mg/mL of L-ASNase onto 2 mg of CNTs at pH 8	34
Figure A1 - Different ammonium sulphate dilutions after reaction with Nessler reagent: A-Blank, B - diluted 100x, C - diluted 25x, D - diluted 10x, S1 - stock solution.....	A1
Figure A2 - Calibration curve for ammonium sulphate quantification.....	A2

List of Tables

Table 1 - L-ASNases commercially available for ALL treatment.	10
Table 2 - Examples of supports and methods used for L-ASNase immobilization.....	16
Table 3 - MWCNTs manufacturer data.	21
Table 4 - Specific surface areas determined by the Brunauer-Emmett-Teller method (S_{BET}) of pristine and functionalized CNTs;.	25
Table 5 - Activity of free L-ASNase (0.086 mg/mL) at different pH values.	30
Table A1 - Ammonium standard solutions used to determine the calibration curve....	A2

Glossary

Abbreviations

ALL	Acute lymphoblastic leukemia
AD	Arc discharge
CNTs	Carbon nanotubes
CVD	Chemical vapor deposition
DTAB	Dodecyl-trimethylammonium bromide
f-CNTs	Functionalized CNTs
MWCNTs	Multi-walled carbon nanotubes
L-Asn	L-asparagine
L-ASNase	L-asparaginase
L-Asp	L-aspartic acid
L-Gln	L-Glutamine
LA	Laser ablation
PZC	Point of zero charge
PEG	Polyethylene glycol
pI	Isoelectric point
S _{BET}	Brunauer-Emmett-Teller specific surface area
SDS	Sodium dodecyl sulfate
SWCNTs	Single-walled carbon nanotubes
TCA	Sulfosalicylic acid
Tris-HCl	Tris(hydroxymethyl)aminomethane

Variables

ABS	Absorbance	
IY	Immobilization Yield	%
m _s	CNT mass	mg
[NH ₄]	Ammonia concentration	μmol.mL ⁻¹
RRA	Relative recovered activity	%
S _{BET}	Brunauer-Emmett-Teller specific surface area	m ² .g ⁻¹
t _r	Reaction time	min

1 Introduction

1.1 Project background

According to the International Agency for Research on Cancer of the World Health Organization, in 2018, 17954537 individuals were diagnosed with cancer (“Global Cancer Observatory”, 2019). Therefore, any effort to prevent the number of deaths verified in 2018 (9555027 people (“Global Cancer Observatory”, 2019)) is critical. One of the many forms of cancer is ALL, a malignant disease induced by cooperative genetic mutations in B- or T-lymphoid precursors (Beckner, 2011). These cells, called undifferentiated blasts or lymphoblasts, will proliferate, but do not mature. Eventually, blasts will fill the bone marrow and progress to different parts of the body (Beckner, 2011). ALL is the most frequent type of leukemia in children up to 14-year-old (Miranda-Filho et al., 2018). The common treatment of ALL includes chemotherapy using the enzyme L-ASNase (Pui et al., 2008), with cure rates ranging 80 to 90% in children, but <10% in elderly and fragile patients (Hoelzer et al., 2016). However, this enzymatic drug, usually produced by bacteria *Escherichia coli* and *Erwinia chrysanthemi*, is related to hypersensitive reactions associated to thrombosis, hyperglycemia, immune suppression and pancreatitis, and minor problems such as allergy, vomiting, coma, headache and lethargy (Ramya et al., 2012).

L-ASNase has another important application in the food industry since this enzyme is able to reduce the acrylamide formation, without flavour changes (Aiswarya & Baskar, 2018). Acrylamide is known to be a probable human carcinogen and is formed by Maillard reaction between L-asparagine and reducing sugars of certain starchy foods at temperatures above 100-120 °C (F. Xu et al., 2016). However, the ideal L-ASNase to be used in the food industry must be stable throughout the food processing and proteolysis (Friedman, 2015).

L-ASNase immobilization is a technique that can overcome the side effects of its application in pharmaceutical industry by preventing the organism proteolytic activity against L-ASNase, increasing enzyme stability and half-life without activity loss (Ulu & Ates, 2017). Increased stability, reuse and easier separation are the main advantages of immobilization that can also be interesting for L-ASNase use in food industry.

The use of nanomaterials in bioprocesses has been rapidly increasing (Riehemann et al., 2009). The nanomaterials structure and composition depends on their characteristics, such as size, shape and surface chemistry (Walkey & Chan, 2012). CNTs are promising supports for enzymes immobilization due to their hydrophobicity, high surface area, functionalization capacity, high bioaffinity and possible low toxicity (Kumar et al., 2017; Schipper et al., 2008).

The knowledge of the interactions between the CNTs and the enzyme is essential for an effective immobilization as well as to design a functional bionanoconjugate with improved properties through possible introduction of target functional groups (Likodimos et al., 2014).

1.2 Contributions of this work and main goals

The L-ASNase immobilization has been studied over several supports such as chitosan, polyethylene glycol (PEG), silica gel and activated carbon, among others (Ulu & Ates, 2017). However, despite of its promising properties, there are few works about L-ASNase immobilization onto CNTs. This way, considering the L-ASNase important applications, it is of high demand to deepen the knowledge about L-ASNase/CNTs bioconjugate under different operating conditions to improve enzyme properties.

The aim of this master thesis is to conduct affinity tests with commercial L-ASNase from *E. coli* and different pristine and functionalized CNTs at different pH values and immobilization times, maximizing the immobilization yield (IY) and the enzyme relative recovered activity (RRA). In the future it is planned to evaluate the enzyme to CNTs mass ratio and the thermal, operational and storage stabilities of the enzyme-CNTs bioconjugate.

This master thesis was developed within the project NanoPurAsp (POCI-01-0145-FEDER-031268), funded by FEDER, through COMPETE2020 - Programa Operacional Competitividade e Internacionalização (POCI), and by national funds (OE), through FCT/MCTES. NanoPurAsp project, which is currently under development, comprises the development of sustainable nanomaterials for the purification of anti-leukemic drugs, including three different Universities. São Paulo State University (UNESP) which is dedicated to the production of recombinant L-ASNase by bacteria fermentation with higher biological activity and less side effects, and Faculty of Engineering of the University of Porto (FEUP) and University of Aveiro (UA) focusing on the development of a cost-effective and sustainable platform for the L-ASNase purification from the fermentation broth using nanomaterials.

1.3 Thesis Organization

This thesis is divided into 8 chapters. In Chapter 1, the main objectives and the background of this work are presented and justified. It provides a guideline to the overall work presented in the further chapters.

Chapter 2 is a review of the literature, positioning the work within the context of existing published reports. This chapter starts with the enzyme presentation, structure and metabolism role. Then, an overview is made about L-ASNase place in food and pharmaceutical industries. This chapter finishes with a synopsis about enzyme immobilization matrices and methods, a

state-of-the-art about supports used in L-ASNase immobilization and a sketch about main features of CNTs and their usage as a carrier.

Chapter 3 is divided into the materials and methods, where an explanation of the methods used and the steps followed are provided, while explaining the formulas considered to discuss the results. Methods of CNTs functionalization and characterization, L-ASNase isoelectric point determination, calibration curve for the determination of L-ASNase activity and of the effect of immobilization time and pH value on the L-ASNase immobilization are described.

In Chapter 4 the results are presented and discussed with the same pattern from the previous chapter. In this chapter, an explanation about the method selection is also given.

Finally, Chapter 5, 6 and 7 give the conclusions of the work presented, limitations and future perspectives and a final appreciation of the developed work, respectively, while chapter 8 lists the references.

2 Literature review and state-of-the-art

2.1 L-ASNase - mechanism, structure and sources

First reported by Lang, in a German journal in 1904 (Pandey et al., 2007), L-Asparaginase (L-ASNase, E.C.3.5.1.1) is an amidohydrolase enzyme that catalyses the conversion of the amino acid L-asparagine (L-Asn) to L-aspartic acid (L-Asp) in two steps. In the first one, the nucleophilic residue of the enzyme is activated by NH_2 , attacking, subsequently, the carbon atom of the amide group in L-Asn generating an intermediate product beta-acyl-enzyme, with the simultaneous release of ammonia. Then, in the second step, the enzyme acts on the ester carbon formed consuming one water molecule and forming L-aspartic acid (Cachumba et al., 2016; Shakambari et al., 2019). The global reaction is showed in Fig. 1.

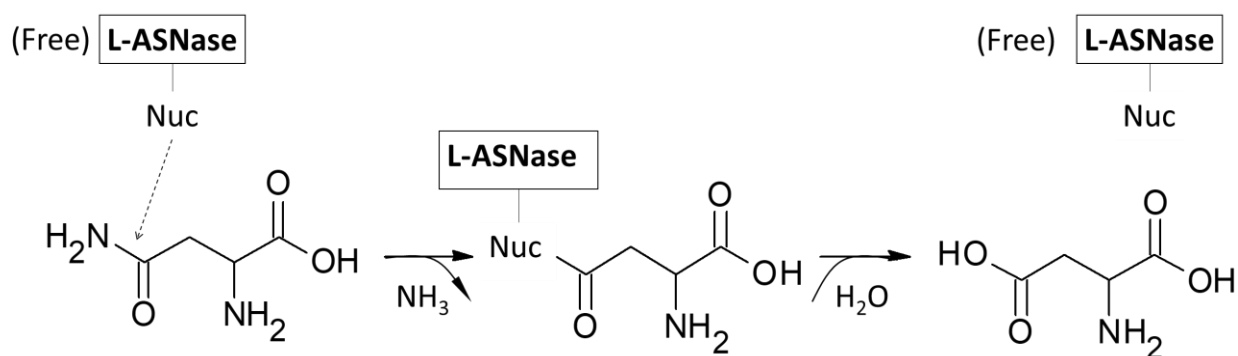


Figure 1 - L-asparaginase reaction mechanism.

The main reserve of ammonia in plants is L-Asn. Hence, it is interesting to note that L-ASNase is widely distributed along plants and microorganisms, while found active in all tissues of herbivores animals and liver of omnivorous animals. There are more types of L-ASNase derived from other living organisms, like mammals, birds and fishes (Lopes et al., 2017), but is absent in all organs of carnivores (Pandey et al., 2007).

Classified by their source organism, the main L-ASNases are bacterial-type L-ASNases, plant-type L-ASNases, and Rhizobial-type L-ASNases (Izadpanah et al., 2018). Submerged fermentation with microorganisms is the most frequent technique used in production of industrial L-ASNase. The factors that influence the production yield are the organism source, the carbon and nitrogen sources, pH, temperature, fermentation time and medium aeration (Lopes et al., 2017).

L-ASNases from *E. coli* are the most used in the market and can be divided into two subclasses, type I and type II, based on their location on the cell. Type I L-ASNases are cytosolic enzymes encoded by *ansA* gene that exhibit low affinity to L-Asn and some specific activity for

L-glutamine (L-Gln), due to the similar structure between these two amino acids (see Fig. 2). Type II L-ASNases, encoded by *ansB* gene, can be encountered in the periplasm and are known to have high specific affinity for L-Asn and low to none specific activity towards L-Gln (Izadpanah et al., 2018; Yun, et al., 2007).

There is a third subclass of L-ASNase from *E. coli*, Isoaspartyl peptidase, expressing some asparaginase activity (Borek et al., 2004), however, since this is not its main reaction, its study has not been further investigated.

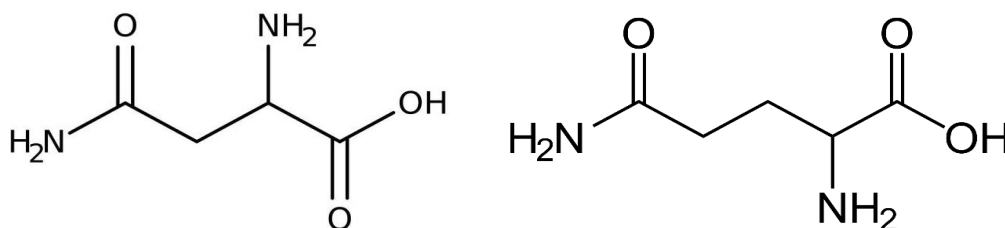


Figure 2 - L-Asp (left) and L-Gln (right) structures.

L-ASNase I is constitutively expressed, being this enzyme related to aspartic acid amino acid family pathway (Ramya et al., 2012; Yun et al., 2007) and can be useful either to use L-Asn as a nitrogen source or to degrade the L-Asn excess accumulated in the cell (Srikhanta, et al., 2013). For example, *Corynebacterium glutamicum* is usually the type of microorganism related to the production and excretion of amino acids. In this gram-positive bacterium, L-ASNase is produced constitutively and its role is to degrade excess L-Asn into L-Asp, that is subsequently converted into L-lysine or L-threonine (Batool, et al., 2016).

On the other hand, type II L-ASNases are mainly expressed underneath nutrient starvation and anaerobic conditions. The expression of this enzyme is regulated by both cyclic adenosine monophosphate receptor protein (CRP) and the oxygen-sensing regulator of fumarate and nitrate reduction (FNR) protein (Jennings & Beacham, 1993). FNR is a transcriptional activator which regulates a number of genes in order to change the metabolism to anaerobiosis (Scott, et al., 1995). L-ASNase II can be expressed to exploit L-Asn as both carbon and nitrogen sources under extreme conditions (Srikhanta et al., 2013). Such role can be emphasized by the fact that CRP regulation occurs in carbon-limited cultures (Narang, 2009).

One major difference between type I and II L-ASNases is the Michaelis Menten constant, K_M , towards L-Asn hydrolysis. Reported apparent K_M from type I is 3.5 mM (Yun et al., 2007), while type II apparent K_M is 11.5 μ M (Swain, et al., 1993). This difference is in accordance with the anti-tumor activity observed in type II L-ASNases due to the higher specific affinity to L-Asn (Yun et al., 2007).

The previous statement illustrates the difference about the affinity to L-Asn between both enzymes. However, L-ASNase I is an allosteric enzyme, so the kinetics do not effectively match the Michaelis-Menten model. The literature reports that L-ASNase I exhibits positive cooperativity with a Hill coefficient (value that defines the cooperativity of substrate binding to the protein) of 2.6 (Yun et al., 2007), which translates into a faster catalysis compared to a kinetics without allosteric mechanisms.

The common active structure of L-ASNase is tetrameric with 222 symmetry, composed by four identical subunits denominated by A, B, C and D (Swain et al., 1993). Each monomer consists of about 326 and 358 amino acids for L-ASNase type I and II, respectively. The strongest interactions are between A-B and C-D subunits establishing two pairs of subunits. In this case, the tetramer can be seen as a dimer of intimate dimers (Swain et al., 1993; Yun et al., 2007). Depending on the enzyme source, another possible structures, such as hexameric, dimeric, and monomeric forms are found when isolated (Batool et al., 2016). An example of both L-ASNase I and II structures, taken from PDB RCSB database (“PDB RCSB homepage”, 2020) with ascension codes 2P2N and 3ECA, respectively, are represented in Fig 3. The active site of the enzyme is located between the N-terminal of subunit C and C-terminal of subunit A and the catalytic activity is only detected in the tetrameric structure (Jaskólski, et al., 2001; LN, et al. 2011).

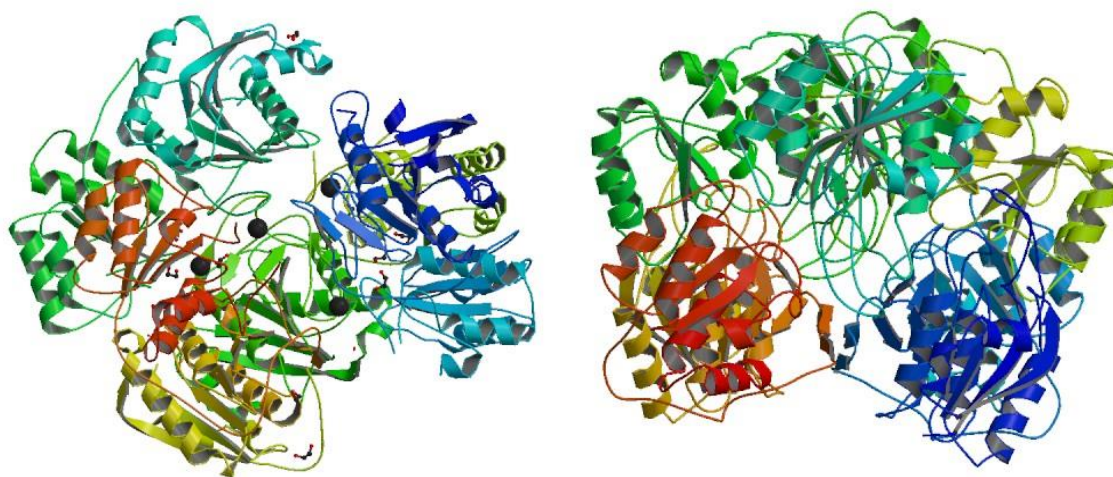


Figure 3 - Crystal structure of *E. coli* L-ASNase I (left) and L-ASNase II (right).

2.2 L-ASNase in food industry

L-ASNase can be used in the food sector for acrylamide mitigation. L-Asn, in the presence of reducing sugars, is the main precursor of acrylamide generation (F. Xu et al., 2016), which is considered a compound that potentially increases the risk of developing cancer according to European Food Safety Authority (EFSA) (“Scientific Opinion on acrylamide in food,” 2016). This reaction, known as Maillard reaction, occurs when starch-rich products like potato chips, French fries, bread or processed cereals are cooked over 120 °C (Di Francesco et al., 2019). This reaction mechanism and the generic amino acid pathway are represented in Fig 4 (F. Xu et al., 2016).

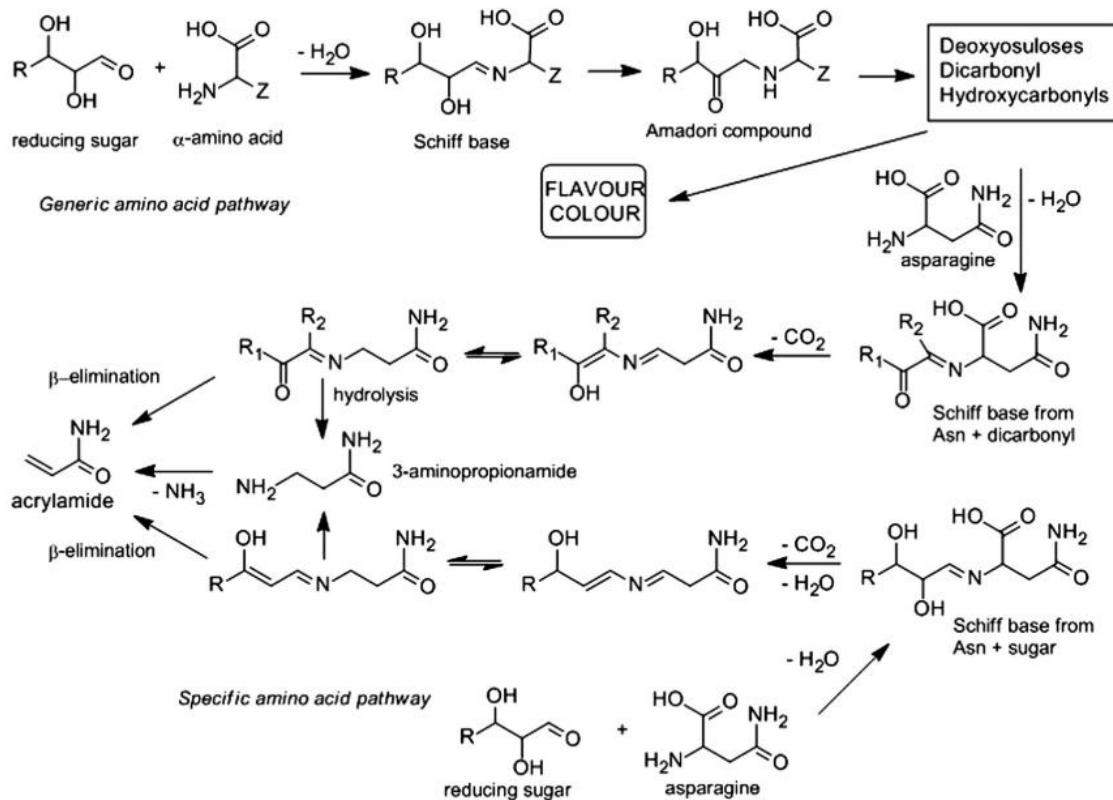


Figure 4 - Generic amino acid pathway and different paths to acrylamide production from L-asparagine. Reprinted with permission from reference F. Xu et al., 2016. Copyright 2016 Elsevier B.V.

Acrylamide is an easy component to detect, since there is a strong relation between the colour of the food crust and the acrylamide content (Surdyk, et al., 2004). Therefore, a pre-treatment of food goods with L-ASNase to consume L-Asn can potentially decrease the amount of acrylamide formed up to 90% without affecting its physical-sensory properties (Liu, et al., 2019; Kumar, et al., 2014). Other alternative is the use of other additives, like sodium chloride, that inhibit the formation of Schiff bases; however, in this case, the food sensory properties are modified (Aiswarya & Baskar, 2018).

Commercial approved L-ASNases to be used in food industries are Acrylaway® from *Aspergillus oryzae* and PreventASe™ from *Aspergillus niger*. The first commercially available

product treated with L-ASNase (PreventASe®), biscuits, was launched in Germany in 2008 (“First ‘Acrylamide-Free’ Biscuits Will Be Launched Germany,” 2007), however, its production at industrial-scale is still being studied.

Since L-ASNase is inactivated by heat and digestion, it should be noticed that it is only active during the L-Asn processing (Muslim et al., 2015). This means that the L-ASNase consumption is unlikely to lead to an allergic reaction, but, on the other hand, it can only be used once (Muslim et al., 2015). Thus, L-ASNase immobilization can be an useful and economic method for its application in food industry, since its immobilization can increase the enzyme thermal stability (Moharam, et al., 2010). Moreover, L-ASNase immobilization allows its use in continuous mode for at least one month, without considerable activity loss, and turns the enzyme more resistant from proteolytic enzymes attack (Muslim et al., 2015).

2.3 L-ASNase in therapeutic sector

2.3.1 L-ASNase as chemotherapeutic agent

Leukemia is, by far, the most common cancer in children until the age of 14, with the estimated number of cases for that age group in 2018 being more than 65000, followed by brain or central nervous system cancers and Non-Hodgkin lymphoma, with around 24000 and 17000 reported cases, respectively (“Global Cancer Observatory,” 2019). Cancer can occur in any body tissue or organ, with leukemia being the cancer of the blood and bone marrow. Leukemia is a consequence of uncontrolled growth and division of some type of blood cells, which will replace healthy blood cells and, eventually, overcrowd the blood (Bozzone, 2009; Felman, 2019). This type of cancer is hard to detect in its early stages, since no unusual growths or nodes are noticeable and early symptoms include fatigue, headaches, fever, chills, or general lack of “well-being” (Bozzone, 2009).

Acute myeloid leukemia (AML), chronic myeloid leukemia (CML), acute lymphoid leukemia (ALL), and chronic lymphoid leukemia (CLL) are the four major types of leukemia (Bozzone, 2009). ALL is the most predominant, accounting to 75% of all diagnosed childhood leukemia cases (Belson, et al., 2007). The cure rates for children, where 80% of the cases occur, are around 90%, but this rate decays to 30-40% for patients aged around 50 (Terwilliger & Abdul-Hay, 2017) and to less than 20% in elderly people (>65 years-old) (Hoelzer et al., 2016).

ALL is originated from genetic lesions in blood-progenitor cells that are differentiated by T-cell or B-cell pathways (Iacobucci & Mullighan, 2017; Pui et al., 2008). These mutations lead to a different lymphoblastic cells proliferation, survival, maturation and accumulation

(Beckner, 2011). The term acute refers to the fast progress of the disease (Felman, 2019). ALL diagnosis is established by the presence of 20% or more lymphoblasts in the bone marrow or peripheral blood (Terwilliger & Abdul-Hay, 2017), therefore a fast and effective approach is needed to recover the cells balance in the blood.

The blasts, or lymphoblasts cells, unlike normal human cells, are auxotrophs for L-Asn, due to their low-to-no level of L-Asn synthetase (Shakambari, et al., 2019). This enzyme catalyses the L-Asn biosynthesis from L-Asp, although it requires a nitrogen source like glutamine (Zhang et al., 2013). Fig 5 shows a scheme of normal blood vessel, where all type of normal cells can be seen (A). (B) represents ALL, where lymphocytes overwhelm the blood, using L-Asn in the blood serum. When L-ASNase (represented by the green “pac-man” shape) is added to the blood serum (C), L-Asn depletion occurs and, while normal cells continue to develop, lymphoblastic cells are arrest in G1-phase, leading to cell apoptosis (Ghasemian et al., 2019).

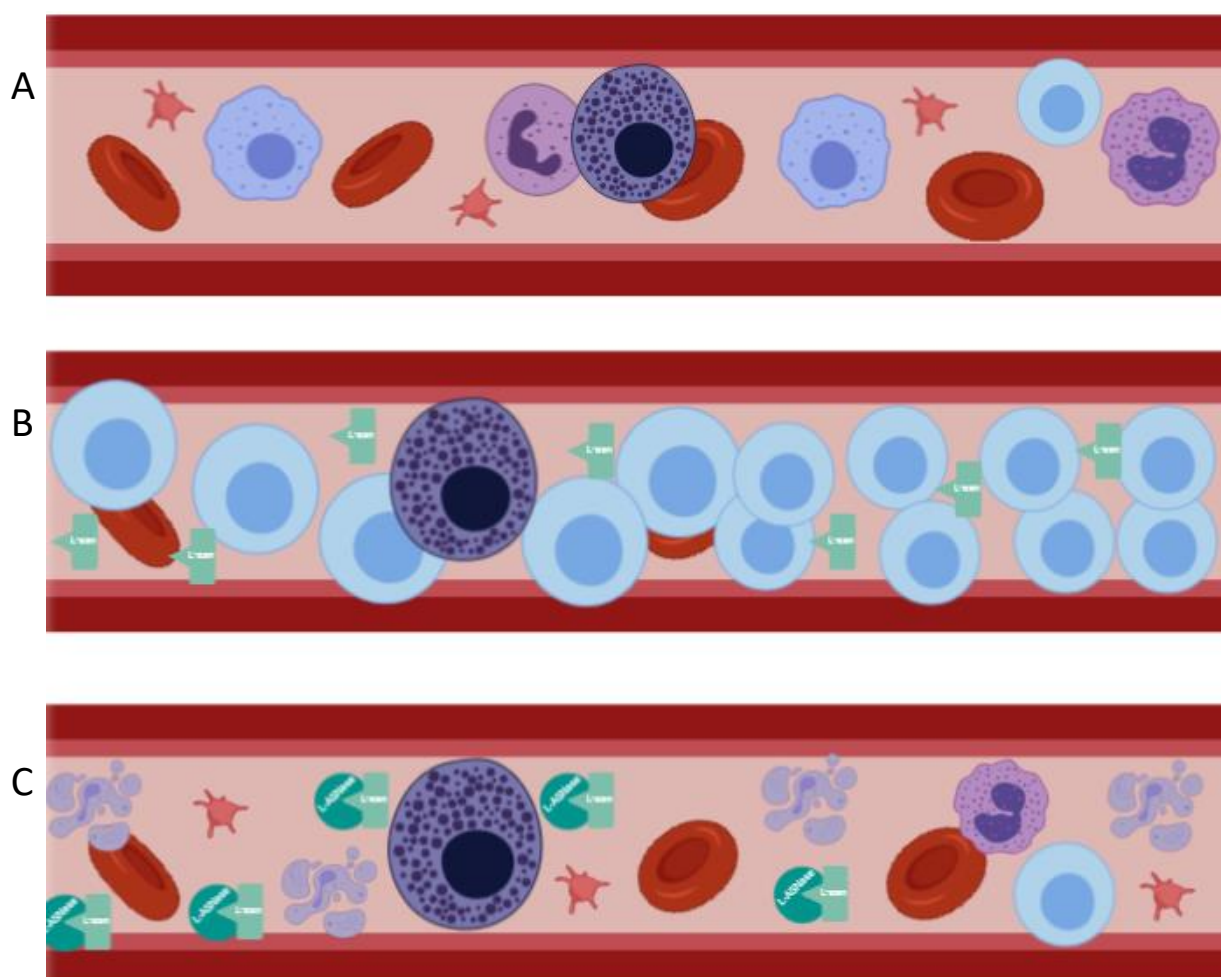


Figure 5 - Schematic example of L-ASNase effect on ALL- A - Normal blood vessel; B - Blood vessel overwhelmed with Lymphocytes; C - Blood vessel from B, after treatment with L-ASNase.

L-ASNase is a widely known therapeutic enzyme used for the treatment of ALL (Piątkowska-Jakubas et al., 2008) in combination with vincristine and a glucocorticoid (Vimal & Kumar, 2017). This enzyme can also be used in the treatment of non-Hodgkin lymphomas (Shakambari et al., 2019b), lymphosarcoma, Hodgkin's disease, acute myelogenous leukemia, acute myelomonocytic leukemia, chronic lymphocytic leukemia, reticulosarcoma and melanosarcoma (Lopes et al., 2017). The use of L-ASNase as a chemotherapeutic agent presents advantages as its biodegradability, non-toxicity and ease of administration (Kamble et al., 2012). It was estimated that L-ASNase production contributed up to 40% of the total worldwide therapeutic enzyme sales in 2009 (Warangkar & Khobragade, 2009), expressing the reputation of this enzyme in the industry.

Currently, there are 3 types of L-ASNases in the pharmaceutical market used for ALL treatment, presented in the Table 1 with their respective cost (Batool et al., 2016; Kloos et al., 2017):

Table 1 - L-ASNases commercially available for ALL treatment.

L-ASNase	Commercial names	Price (\$/vial)	Units (IU)
<i>E. coli</i> Native L-ASNase	Colaspase; Elspar; Kidrolase; Sprectila	77	5000
<i>E. coli</i> PEGylated L-ASNase	Oncaspar; PEG-asparaginase; Pegasparagasum	1387	3750
<i>Erwinia chrysanthemi</i> native L-ASNase	Crasnitin; Crisantaspase; Elspar; Erwinaze; Kidrolase	850	10000

At the moment, *E. chrysanthemi* PEGylated L-ASNase, under the commercial name of Asparec, is under phase 1 clinical trials ("Phase I Study of mPEG-R-Crisantaspase Given IV " 2015). PEGylation is a modification induced by covalent attachment of monomethoxypolyethylene glycol (PEG) to native L-ASNase, in order to increase enzyme serum half-life and decrease immunogenicity (Ettinger et al., 1997). *E. chrysanthemi* L-ASNase is generally administered in patients who experienced *E. coli* L-ASNase allergic reactions (Wacker et al., 2007), since it was found that there is no cross-reactivity between these enzymes (Narta et al., 2007).

Although presenting similar treatment mechanisms, these commercial formulations exhibit different characteristics. For example, via intramuscular injection, native *E. coli* and *E. chrysanthemi* L-ASNases have half-lives of 1.28 and 0.6 days, respectively, while PEGylated L-ASNase exhibits an half-live of 5.73 days (Asselin et al., 1993; Ettinger et al., 1997). This means that treatment with PEG-asparaginase needs less doses compared to native enzyme treatment (W. Liu et al., 2016), which can help in reducing allergic reactions.

One of the most cost-efficient protocols used in ALL treatment has a total cost about \$29000, being the cost of the L-ASNase medication alone around \$13000 considering no L-ASNase waste or hypersensitivity. This is the best-case scenario. If each L-ASNase vial is used only one time, this medication cost is raised to more than \$47000 (Kloos et al., 2017).

2.3.2 Side effects of L-ASNase as a therapeutic drug

Although the L-ASNase introduction has been a great advance in ALL treatment, there are some recognized side effects of using this bacterial enzyme, namely hypersensitivity leading to allergic reactions such as skin rashes, respiratory disorders, low blood pressure, pain, oedema, loss of consciousness and anaphylaxis (Lopes et al., 2017; Pieters et al., 2011). Hyperlipidaemia, pancreatitis, thromboembolism and central nervous system thrombosis, glucose intolerance and coagulopathy are other of the many reported severe side effects that are directly related to L-ASNase treatment protocols (Dinndorf et al., 2007; Schmiegelow et al., 2016). Hypersensitivity reactions are more common in paediatric patients than with adults (Burke & Rheingold, 2017).

It should be also noted that, in the beginning, the L-ASNase was administered only via intramuscular injections, but currently it is also administered intravenously, which triggers hypersensitivity reactions earlier in the treatment (Burke & Rheingold, 2017). Patients are also more likely to have a side reaction at their second or third administered dose (Browne et al., 2018) On the other hand, being the L-ASNase of bacterial origin and a high molecular weight enzyme, it is naturally rejected by the body's immune system (Ulu & Ates, 2017).

A strategy to reduce side effects and improve L-ASNase therapeutic effect has been studied through its chemical modification and physical integration with several support carriers such as PEG (PEG-asparaginase), liposomes and albumin (Vidya et al., 2017; Ulu & Ates, 2017).

2.4 Enzymes immobilization

The immobilization of enzymes refers to their confinement on support materials, with the objective of making them more stable and allowing their reuse, while retaining or improving their catalytic activities (Mohamad et al., 2015). This process brings advantages like enzymatic recovery and reuse, contributing to the reduction of process costs (Gupta et al., 2011). Additional immobilization advantages are increased enzyme stability in a wider pH and temperature range, for solvents, contaminants, and impurities and the ability to quickly stop the reaction by easily enzyme removal from the solution, which can decrease the product contamination (Elnashar, 2010).

Enzyme immobilization is already a common process in the nature, since some enzymes are naturally attached to cell cytoskeleton, membrane and organelle structures, stabilizing the enzyme while maintaining its activity (Homaei et al., 2013). The commercial approved PEG-asparaginase is already an enzymatic immobilization process, reporting 18% of hypersensitivity reactions, compared with 32% for native L-ASNase (Ulu & Ates, 2017).

There are several supports used in enzyme immobilization, which can be divided by their chemical characteristics and origin (Fig 6, adapted from Elnashar, 2010).

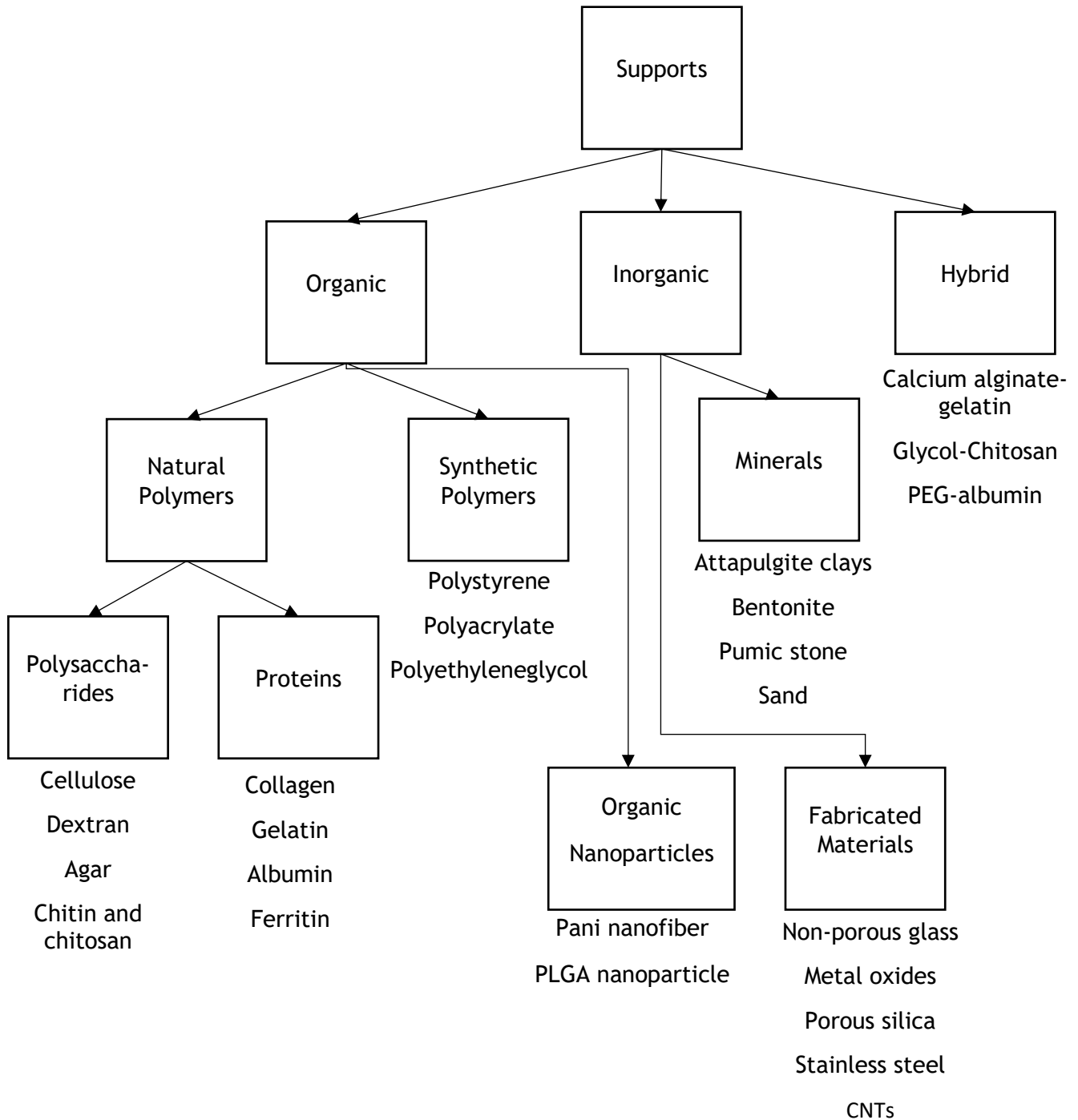


Figure 6 - Different matrices used for enzyme immobilization (adapted from Elnashar (2010)).

An ideal carrier should be biocompatible, easily accessible, cheap, stable, and suitable for regeneration. The organic supports can be divided into natural and synthetic. Natural supports are the most common used for enzyme immobilization, being biocompatible, biodegradable,

and inexpensive. Although synthetic polymers come from non-renewable petroleum resources, they have the advantage that their shape, form, porosity, pore diameter, polarity, hydrophobicity and surface functional groups can be controlled during their synthesis (Ulu & Ates, 2017). From all matrices, nanoparticles display the highest surface areas and largest porosities, providing a high enzyme loading and facilitating the accessibility of the substrate to the active sites (Ulu & Ates, 2017). Compared with organic ones, inorganic supports have few functional groups, limiting the enzyme attachment, but exhibit high chemical, physical, and biological resistance. In addition, inorganic materials have uniform pore sizes, large surface areas, and are easily functionalized (Tran & Balkus, 2011). Finally, there is a last type of supports that combines the properties of both natural and synthetic ones, the hybrid supports (Ulu & Ates, 2017).

There are several immobilization methods, being classified mainly as chemical (covalent attachment and crosslinking), where covalent bonds between the enzyme and the carrier are established, and physical (divided into adsorption, entrapment and encapsulation), where weak interactions are formed (Homaei et al., 2013). The establishment of the immobilization process should take into account the retention of the enzyme's active conformational arrangement and also its catalytic flexibility (Clark, 1994). As every enzyme and process have different properties that require distinct support characteristics, there is no better method or immobilization support, each presenting its advantages and disadvantages (Homaei et al., 2013). Fig 7 (Nguyen & Kim, 2017), schematize the differences between covalent bonding, cross-linking, adsorption and entrapment/encapsulation methods.

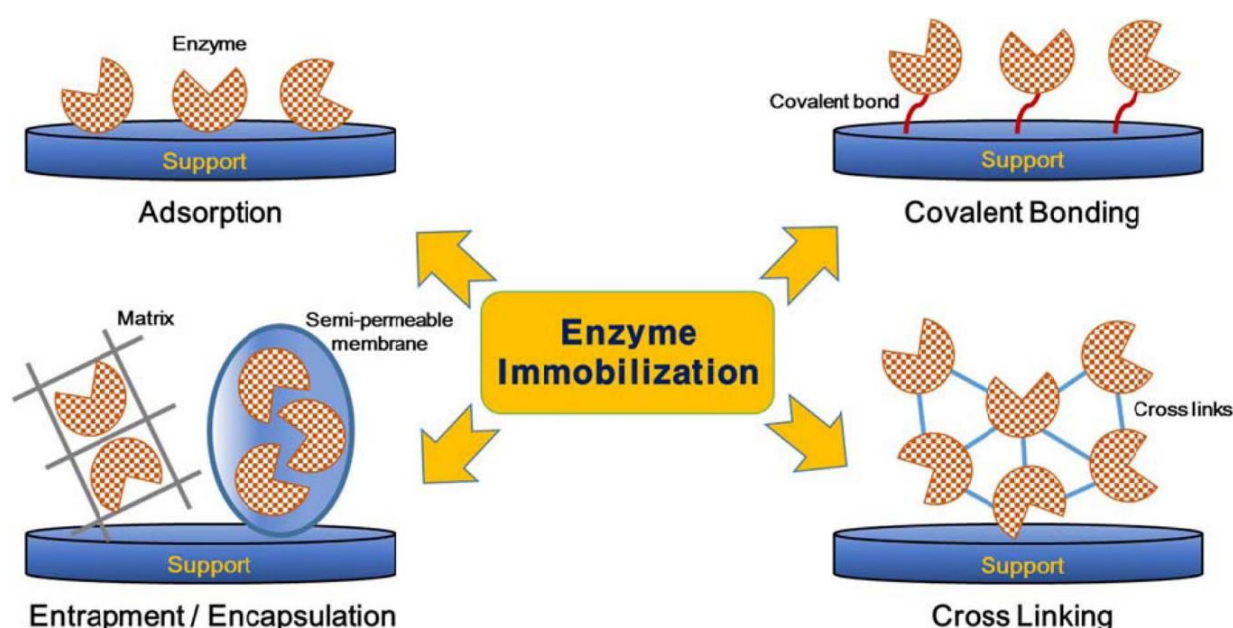


Figure 7 - Schematic representation of different enzyme immobilization methods. Adapted from Nguyen & Kim, 2017. Copyright 2017, The Korean Vacuum Society.

Adsorption is the simplest, cheapest and most effective method, but it can lead to reversible reactions and surrounding media contamination by the enzyme due to the weak driving forces involved, whether being hydrophobic or electrostatic interactions (Homaei et al., 2013; Tran & Balkus, 2011). Adsorption of enzymes may result into conformational changes and denaturation of proteins. Additionally, there is no control on packing density of immobilized enzymes and their activity can be reduced by excessive crowding (Homaei et al., 2013), being the carrier-to-enzyme ratio and the immobilization time important factors to consider in order to avoid that drawback.

The covalent bonding, or bioconjugation, ensures a more stable enzyme attachment on the support. Covalent bonds usually occur between the amino acid chain in the arginine, lysine, aspartic acid and histidine residues (Brumano et al., 2019) and, for example, activated acid or ester groups of the support (Fernandes et al., 2018; Homaei et al., 2013). The major disadvantage of the covalent attachment is the enzyme activity loss, however, usually there is an improvement of thermal and environmental stabilities of the enzyme (Suma et al., 2016). This type of immobilization is common on bioreactors, due to prolonged periods of use and recovery with low enzyme release onto the product (Tran & Balkus, 2011). Since inorganic supports usually have limited biocompatibility and lower affinity to biomolecules, in order to create a covalent bond between the enzyme and an inorganic support, a cross-linking agent, such as glutaraldehyde, is frequently required (Zdarta et al., 2018).

The entrapment immobilization method consists of restricting the enzyme in a two-step mechanism within a polymeric network which allows only the passage of substrates and products (Nguyen & Kim, 2017). In the first step, the enzyme is mixed with the monomer solution, and in the second one, the polymerization of the monomer solution occurs, physically trapping the enzyme. This method improves the enzyme stability, minimizes the enzyme leaching and permits the optimization of the enzyme microenvironment by modifying the encapsulation material to have the optimal pH and polarity (Nguyen & Kim, 2017). This method drawbacks are the mass transfer resistances with a higher polymerization extension, needing a balance between the mass transfer resistance and the enzyme leakage, low enzyme loading capacity and corruption of the support with polymerization reactions (Nguyen & Kim, 2017).

Encapsulation is the wrapping of biological components within different forms of semi permeable membranes. As in entrapment, proteins and enzymes cannot out move in or out of the capsule, only small substrates and products are allowed (Tran & Balkus, 2011). The main difference is the freedom of movement within the membrane space, that also enables co-immobilization. Problems of encapsulation include membrane rupture and mass transfer resistance. Biological cells, such as red blood cells, can be used as membranes (Elnashar &

Hassan, 2014). Table 2 shows some examples of supports and immobilization methods already used for L-ASNase immobilization.

Table 2 - Examples of supports and methods used for L-ASNase immobilization, adapted from Ulu & Ates (2017)

Support nature	Support material	Immobilization method	Ref
Natural	Albumin	Cross-linking	Poznansky et al, 1982
	Chitin and chitosan	Covalent binding	Moharam et al., 2010
	Insulin	Chemical modification	Tabandeh & Aminlari, 2009
	Erythrocytes	Encapsulation	Min et al., 2009
	Fatty acids	Covalent binding	Ashrafi et al., 2013
Synthetic	Polyurethane foam	Adsorption	Kattimani et al., 2009
	PEG	Covalent binding	Soares et al., 2002
	Carboxymethyl cellulose	Covalent binding	Moharam et al., 2010
Nano	Poly(D,L-lactide-co-glycolide) nanospheres	Encapsulation	Wolf, et al., 2003
	Hydrogel-magnetic nanoparticles	Entrapment	Teodor, et al., 2009
	Polyaniline nanofiber	Covalent binding	Ghosh, et al., 2012
Inorganic	Silica gel	Adsorption	Ashrafi et al., 2013
	Sephadex G-50	Entrapment	Ashrafi et al., 2013
	Activated carbon	Covalent binding	Moharam et al., 2010
	Celite	Covalent binding	Moharam et al., 2010
Hybrid	PEG-chitosan and Glycol-chitosan	Covalent binding	Teodor et al., 2009
	Calcium alginate-gelatin	Cross-linking	Youssef & Al-Omair, 2008
	Calcium-alginate/multi-walled carbon nanotube beads	Encapsulation	Ulu et al., 2020

2.5 Carbon nanotubes

CNTs are one of the allotropes of carbon. Their tubular structure, made of graphite, was first reported by Iijima (1991). Divided into single-walled (SWCNTs) and multi-walled carbon nanotubes (MWCNTs) (Fig 8) (Saifuddin et al., 2013), CNTs are promising immobilization supports for enzymes due to their large surface area to volume ratio, relatively small diameter, hollow structure, bioaffinity and hydrophobic nature (R. Xu et al., 2015). CNTs have lengths in the order of μm and diameters up to 100 nm.

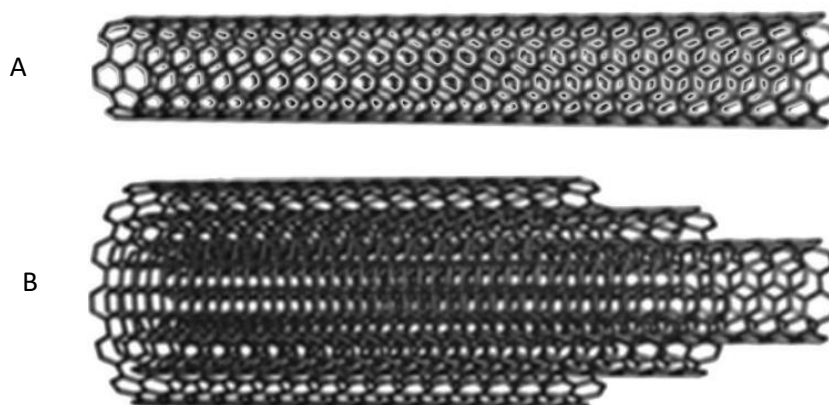


Figure 8 -Structure of (A) SWCNTs and (B) MWCNTs, adapted from Saifuddin et al. (2013).

SWCNTs structure consists of rolled-up tubular shell of a graphene sheet, composed of benzene type hexagonal rings of carbon atoms. Despite the simple structure of SWCNTs, which guarantees an extremely high surface area, their synthesis is more difficult, high purity is harder to achieve and requires more control over growth and atmospheric conditions. SWCNTs are not fully dispersed, and tend to be curved, due to their ease of twisting. On the other hand, SWCNTs are easy to characterize (Saifuddin et al., 2013).

In turn, MWCNTs consist of multiple layers of graphene rolled-up in a concentric way, are easier to synthesize, achieving high purity levels with a lower chance of creating defects. The complex structure gives stiffness to MWCNTs. Lower production costs and easier dispersibility are the advantages of these CNTs, which are harder to characterize (Saifuddin et al., 2013).

CNTs are synthesized by methods such as arc discharge (AD), laser ablation (LA) and chemical vapor deposition (CVD). The first two lead to almost perfect nanotube structures, but require temperatures above 1700 °C, need to use solid-state carbon precursors and large amounts of by-products are formed (Kumar et al., 2017; Saifuddin et al., 2013). CVD uses pyrolysis to form hydrocarbon gases, and catalyst particles for CNTs nucleation. This is the

method used for both SWCNTs and MWCNTs large scale production and requires temperatures up to 800 °C (Kumar et al., 2017; Saifuddin et al., 2013).

2.5.1 Immobilization of biomolecules on CNTs

Immobilization of biomolecules onto CNTs can be carried out by many different strategies, namely non-covalent (direct physical adsorption, adsorption onto CNTs functionalized with biomolecules, polymers or surfactants and layer-by-layer deposition) and covalent attachment (with or without cross-linkers use) (Silva et al., 2014; J. Wang, et al., 2006).

Adsorption is the most used method due to its simplicity and for preserving both the immobilized biomolecules conformational structure and CNTs mechanical and electronic properties (Feng & Ji, 2011). The physical adsorption can occur via π - π interactions (using aromatic compounds or polymers), electrostatic interactions, and hydrogen bonds between CNTs and biomolecules. The main challenge of this method is to prevent the biomolecules detachment from the CNT surface (Zhou et al., 2019). To improve the bonding forces, the CNTs can be functionalized with biomolecules such as chitosan, polymers such as polyvinyl pyrrolidone (PVP) and poly-styrene sulfonate (PSS), or surfactants like sodium dodecyl sulfate (SDS) and dodecyl-trimethylammonium bromide (DTAB)(Mohammadi et al., 2015; Hu et al., 2009). In layer-by-layer deposition, layers of enzyme and materials of opposite charges are alternatively formed on top of each other on a solid support with washing steps between them (Nguyen & Kim, 2017).

In order to increase the CNTs compatibility with biomolecules, such as enzymes, some modifications that permanently or reversibly change their chemical properties can be used (Zhou et al., 2019). These modifications are made through their functionalization, being carboxylate, polyethylene glycol, amine, sidewall amine, polyetherimide and sulfhydryl some of the many surface groups that can be generated (R. Li et al., 2013; Zhou et al., 2019). This process can decrease some intrinsic properties of CNTs. Enzyme immobilization on functionalized CNTs can be further extended using covalent binding with or without cross linkers, such as 1-ethyl-3-(3-dimethylaminopropyl)carbodiimide (EDC) (Gao & Kyrtziz, 2008).

In addition to food and pharmaceutical applications, the immobilization of enzymes onto CNTs can also have other biotechnological uses, namely in biosensing and biofuel cells industries. CNT-based sensors exhibit higher sensitivities, lower detection limits and faster electron transfer kinetics than traditional carbon electrodes (Feng & Ji, 2011). L-ASNase immobilized onto CNTs can be used as biosensor to detect L-Asn levels in both clinical and food matrices. This technology is based on the pH change produced by ammonium ions generated during the asparagine hydrolysis (Ulu & Ates, 2017).

Due to its properties, CNTs also have potential to be used in protein purification processes. Mubarak et al. (2011) demonstrated that pristine CNTs are able to replace a hydrophobic interaction chromatography, whereas CNTs functionalized with carboxylic acid groups (f-CNTs) behave like an ion exchange chromatography process during the purification of a protein from skim latex serum. This can be a huge step in reducing the overall costs of L-ASNase and other enzymes purification, since the downstream processes are responsible for around 80% of total production costs, and being the chromatographic processes some of the most expensive purification steps (Lopes et al., 2017; Vimal & Kumar, 2017).

2.5.2 CNTs toxicity

CNTs toxicity is one of the major concerns of their applying in the diagnostic, as biosensor, or therapeutic areas, as mediators or drug nano-carriers. The data about CNTs toxicity is contradictory, with some reports expressing CNTs good biocompatibility, but many others reporting them as a potential health problem (Li et al., 2009).

Monteiro-Riviere et al. (2005) tested pristine MWCNTs toxicity in human epidermal keratinocytes and reported an irritation response from the cells. On the other hand, Liu et al. (2012) reported no major changes in the tissues after intravenous injection of pristine MWCNTs in rats, with the exception of lung tissue, concluding that MWCNTs can cross among the blood vessel walls to move into the lung tissue, inducing lung toxicity. Barillet et al., (2010) tested in vitro cytotoxicity of different nanoparticles (CNTs, TiO₂ and SiC) in lung, liver and kidney cells. The authors reported that the CNTs cytotoxicity does not depend on their length or on the presence of metallic impurities, such as Fe; the sensitivity of lung cells towards CNTs is due to their affinity with a pulmonary surfactant, which increases with the contact time between cells and CNTs.

The CNTs functionalization has been reported as promising in reducing their toxicity. Guo et al., 2007 tested glucosamine functionalized MWCNTs in mice via intraperitoneal injection and reported no severe acute toxicity responses, due to the improved biocompatibility of modified CNTs. R. Li et al. (2013) verified carboxylate (COOH), polyethylene glycol (PEG), amine (NH₂), sidewall amine (sw-NH₂), and polyetherimide (PEI)-modified MWCNTs cytotoxicity in human bronchial epithelium and human monocytic cell cultures. They stated that the carboxylation decreased the pulmonary fibrosis extend when compared to pristine MWCNTs, while positively functionalized CNTs induced lung fibrosis. With these results, it was concluded that the surface charge plays an important role in the lung fibrotic potential of functionalized CNTs. Schipper et al., 2008, in a pilot study, reported no toxicity evidence during 4 months after injection of oxidized and non-oxidized PEG functionalized SWCNTs into mice bloodstream.

With the lack of cell toxicity reported, functionalized CNTs are potential supports for L-ASNase immobilization for use in both pharmaceutical and food industries.

3 Materials and methods

3.1 Materials

E. coli L-ASNase II (> 96,0% purity) 10000 IU, lyophilized with no additives and with 269 IU/mg (ENZ-287) of specific activity was supplied by Deltaclon S.L., Spain.

Non-functionalized multi-walled CNTs (MWCNTs) were purchased from NTP Shenzhen Nanotechnologies Co. Ltd, presenting the manufacture advertised characteristics shown in Table 3.

Table 3 - MWCNTs manufacturer data.

Type of CNTs	Label	Diameter Range (nm)	Length (μ m)	Purity (%)	Ash (wt %)	Specific surface area range (m ² /g)
MWCNT-10	CNT <10	<10	> 5	> 97	< 3	250 - 500
L-MWCNT-1020	CNT 10-20	10-20	> 5	> 97	< 3	100 - 160
L-MWCNT-2040	CNT 20-40	20-40	> 5	> 97	< 3	80 - 140
L-MWCNT-60100	CNT 60-100	60-100	> 5	> 97	< 3	40 - 70

L-Asn ($\geq 99.0\%$), tris(hydroxymethyl)aminomethane (TRIS) ($\geq 99.0\%$) and disodium hydrogen phosphate ($\geq 99.0\%$) were purchased from VWR International, LLC. Trichloroacetic acid (TCA) ($\geq 99.0\%$) was obtained from J.T. Baker. Citric acid ($\geq 99.5\%$) and Nessler's reagent (dipotassium tetraiodomercurate (II)) were supplied by Merck Chemical Company (Germany). Sodium hydroxide ($\geq 98.0\%$) and hydrochloric acid (37%) were bought from Sigma-Aldrich.

3.2 Methods

3.2.1 General solutions

Tris-HCl 50 mM pH 8.6 buffer was prepared by dissolving 0.6057 g of tris(hydroxymethyl)aminomethane in distilled water until 100 mL, adjusting the pH to 8.6 with HCl 0.1 M.

TCA 1.5 M solution was prepared by adding 19.067 g of solid sulfosalicylic acid (TCA) dihydrated to distilled water up to a total volume of 50 mL.

L-asparagine 181 mM solution was prepared by adding 24 mg of L-asparagine to 1 mL of a buffer solution at the desired pH.

The buffer solutions of pH 4.0, 6.0 and 8.0 were prepared using a citrate/phosphate buffer 50 mM, while a 50 mM carbonate buffer was used for pH value of 9.0.

3.2.2 MWCNTs functionalization

Hydrothermal oxidation of the pristine MWCNTs was performed in a Teflon-lined stainless steel autoclave using a 0.5 M HNO₃ aqueous solutions at 200 °C, as described elsewhere (Marques et al., 2010). Briefly, 0.2 g of CNTs was added to 75 mL of a HNO₃ aqueous solution. After being sealed, the vessel was put into an oven at 200 °C for 2 h. Then, the CNTs were recovered, rinsed with water until neutrality, and dried overnight at 120 °C.

3.2.3 Characterization of CNTs

The Brunauer-Emmett-Teller (BET) specific surface area (S_{BET}) of every type of CNTs used was determined through the N₂ adsorption data at -196 °C in the relative pressure range 0.05-0.20, using a Quantachrome NOVA 4200e apparatus. The pH of the point of zero charge (PZC) of the MWCNT samples was determined by using a drift method described elsewhere (Rivera-Utrilla, et al., 2001).

3.2.4 Determination of isoelectric point

The isoelectric point of L-ASNase was determined by measuring the zeta potential of aqueous solutions of L-ASNase (0.086 mg/mL) in a wide range of pH values. To adjust the pH, aqueous solutions of NaOH and HCl 0.01 M were used.

The results were acquired by the equipment Malvern Zetasizer Nano ZS (Malvern Instruments Ltd.) at room temperature (25 °C) and using an appropriate cell to perform this experiment. The zeta potential was read at least 20 times and the test was performed in triplicate.

3.2.5 L-ASNase activity measurement

Enzyme specific activity was quantified using the Nessler method. Nessler method is a simple, fast and cheap way to determine the amount of ammonia in a solution, recognized by the FDA for pure L-ASNase formulations (Magri et al., 2018). The Nessler reagent reacts with ammonia providing a characteristic yellow-to-brown reaction mixture that can be quantified by spectrophotometry (Magri et al., 2018) at 436 nm.

For L-ASNase activity measurements, 50 μL of free native ASNase or of each supernatant or 2 mg of ASNase/MWCNTs conjugate (immobilized) was added to an eppendorf containing 50 μL of 189 mM L-asparagine solution (substrate), 450 μL of distilled water and 500 μL of Tris-HCl 50 mM. The mixtures were incubated for 30 min at 37 $^{\circ}\text{C}$ under stirring. After incubation time, the enzymatic reaction was stopped by adding, in the fume hood, 250 μL of TCA 1.5 M. Subsequently, for the immobilized enzyme, the eppendorfs were again centrifuged at 112 G for 10 minutes to separate the material from the solution. Then 100 μL of supernatant of each sample were transferred to Falcon tubes and mixed with 2.15 mL of distilled water and 250 μL of Nessler reagent. A blank containing 2.25 mL of water and 250 μL of Nessler reagent was prepared for control. After 30 min of incubation at room temperature, absorbance was measured at 436 nm in the double beam spectrophotometer.

In order to quantify the amount of ammonia in the solutions, a calibration curve between the ammonia concentration and the absorbance at 436 nm was determined. For that, an ammonium stock solution (SS) (8.5 mg/mL), was prepared adding 3.098 g of ammonium sulphate to 100 mL of distilled water. The standard solutions P1 to P10 were then prepared by dilutions of SS according to the values presented in appendix 1.

250 μL of Nessler reagent were added to all the standard solutions and after 30 minutes of incubation, the absorbance at 436 nm of each solution was read in a JASCO V-560 UV-Vis double beam spectrophotometer.

L-ASNase activity was determined through equation 1, since it is defined that a unit of L-ASNase activity (U) corresponds to the amount of enzyme that releases 1 μmol of ammonia from L-asparagine per minute at 37 $^{\circ}\text{C}$.

$$L - ASNase \ activity \left(\frac{U}{L} \right) = \frac{[NH_4^+] \left(\frac{\mu\text{mol}}{\text{mL}} \right) \times V_{Nessler}(\text{mL}) \times f_d}{t_r(\text{min})} \quad (1)$$

where $V_{Nessler}$ is the volume of the Nessler solution, f_d is the sample dilution factor taking into account the volume of supernatant kept after the first centrifugation, the final solution volume in the eppendorf and the volume transferred to the Falcon tube. Finally, t_r is the reaction time.

For immobilized L-ASNase, the enzyme activity needs to take into account the mass of support used. Consequently, it can be calculated as shown in equation 2.

$$L - ASNase \ activity \left(\frac{U}{g} \right) = \frac{[NH_4^+] \left(\frac{\mu\text{mol}}{\text{mL}} \right) \times V_{Nessler}(\text{mL}) \times f_d}{t_r(\text{min}) \times m_s(\text{g})} \quad (2)$$

where m_s is the mass of support.

3.2.6 Optimization of L-ASNase immobilization

The L-ASNase immobilization by adsorption onto different CNTs was studied by adding 2 mg of each CNTs to 200 μ L of a 0.086 mg/mL L-ASNase solution in an appropriate buffer, varying the respective pH value (4.0, 6.0, 8.0 and 9.0).

The immobilization was performed by stirring the mixtures during a certain period of time in a multifunctional tube rotator (Grant Instruments Lda., model PTR-35), followed by samples centrifugation at 112 G for 10 min to separate the nanotubes from the supernatant. The contact time was optimized at the selected best pH by performing the immobilization during different periods of time (30, 60, 120 min). For each assay duplicate runs were made.

Relative recovered activity (RRA, %) of the immobilized L-ASNase was considered as the ratio between activity of the immobilized enzyme and the maximum theoretical activity that would exist if the free enzyme was totally immobilized, considering no yield lost, and was calculated by Equation 3.

$$RRA (\%) = \frac{\text{Immobilized L-ASNase activity } \left(\frac{U}{g}\right)}{\text{Maximum L-ASNase activity } \left(\frac{U}{g}\right)} \quad (3)$$

where

$$\text{Maximum L-ASNase activity } \left(\frac{U}{g}\right) = \frac{[NH_4^+]_{free L-ASNase} \left(\frac{\mu mol}{mL}\right) \times V_{Nessler} (mL) \times f_d}{t_r (min) \times m_s (g)} \quad (4)$$

The immobilization yield (IY, %) was calculated by Equation 5, being defined as the difference between the free enzyme activity before immobilization and the activity of the enzyme remaining in the supernatant after immobilization, divided by the free enzyme activity before immobilization.

$$IY (\%) = \frac{\text{Free L-ASNase Activity } \left(\frac{U}{mL}\right) - \text{Supernatant L-ASNase Activity } \left(\frac{U}{mL}\right)}{\text{Free L-ASNase Activity } \left(\frac{U}{mL}\right)} \times 100 \quad (5)$$

4 Results and discussion

4.1 Characterization of carbon nanotubes

CNTs have been reported as an effective support for enzymes immobilization, mainly due to their high specific surface area and high enzyme loading capacity (Feng & Ji, 2011; Shim et al., 2002; L. Wang et al., 2010). Additionally, CNTs surface can be easily functionalized, tuning their properties towards specific applications and enhancing their efficiency as enzyme support. In this way, the pristine CNTs were oxidized with HNO₃ (0.5 M) in order to generate materials with large amounts of surface oxygen groups, namely carboxylic acids, anhydrides, quinones, phenols, etc (Shim et al., 2002).

There are at least two characteristics of the support that can be considered important to study the immobilization of enzymes: the point of zero charge (PZC), i.e., the pH at which the net charge of total particle surface is equal to zero, and the specific surface area (S_{BET}). The PZC of the pristine CNTs was previously determined by other members of the research team using a drift method being around 7 (Silva et al., 2014), a value close to other CNTs reported in literature (7.3) (Hou et al., 2019). The introduction of surface acid groups through oxidation of pristine CNTs lead to a PZC of functionalized CNTs (f-CNTs) around 3-4 (Silva et al., 2014).

The S_{BET} of pristine and functionalized CNTs determined by the BET method through N₂ adsorption-desorption isotherms are displayed in Table 4, together with the ones reported by the manufacturer.

Table 4 - Specific surface areas determined by the Brunauer-Emmett-Teller method (S_{BET}) of pristine and functionalized CNTs; *range reported by the manufacturer.

CNT	Functionalization	Specific surface area range* (m ² /g)	S_{BET} (m ² /g)
CNT <10	Pristine	250 - 500	350
	-COOH	-	408
CNT 10-20	Pristine	100-160	104
	-COOH	-	123
CNT 20-40	Pristine	80-140	67
	-COOH	-	85
CNT 60-100	Pristine	40-70	30
	-COOH	-	33

As expected, as the diameter of the CNTs increases, there is a decrease in their surface area. The hydrothermal oxidation treatment led to an increase in the surface area of CNTs, explained by the creation of defects on the CNTs sidewalls along with the opening of the CNTs end caps, causing an increase in the porosity, as reported by Silva et. al (Silva et al., 2014). The same source reports that this type of functionalization produces CNTs mainly with carboxylic acid surface groups. Therefore, an increase in the acidity of the CNTs surface and a decrease of the PZC to lower values is expected after treatment with HNO_3 . One additional characteristic was observed after the centrifugation step. An easy separation from the aqueous solution is an intuitive advantage of protein immobilization. However, as presented in Fig 9, after centrifugation, some pristine CNTs, especially the CNT 20-40 and CNT 60-100 ones tend to stay in the solution, hindering the separation process.

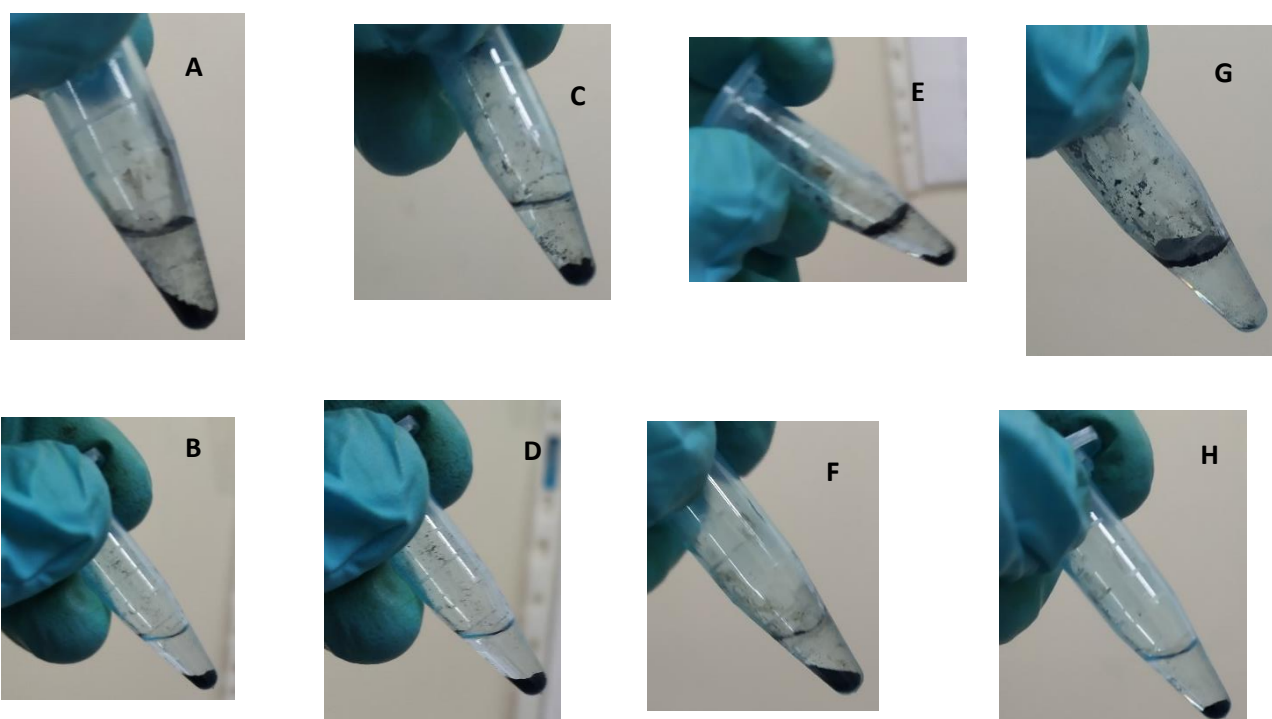


Figure 9 - CNTs after centrifugation: A - CNT <10; B - f-CNT <10; C - CNT 10-20; D - f-CNT 10-20; E - CNT 20-40; F - f- CNT 20-40; G - CNT 60-100; H - f-CNT 60-100

This was expected, due to the hydrophobic characteristics of pristine MWCNTs. However, this problem can be easily overcome by switching from a centrifugation to a filtration step. f-CNTs demonstrated an easier and faster separation by centrifugation, as their additional functional groups contribute to a decrease of hydrophobicity.

4.2 Determination of L-ASNase isoelectric point

The isoelectric point (pI) is the pH of a solution at which the net charge of the enzyme becomes zero. So, the pI determination allows to verify the enzyme charge at a given pH value, being, this way, an important parameter to comprehend the results. When the solution pH value is equal to pI, the enzyme shows an absence of inter-particle repulsive forces, being the enzyme more compact and hydrophobic and, consequently, less soluble and stable (Salgin et al., 2012). The knowledge of the L-ASNase pI and the CNTs PZC allows to understand the type and forces of interaction between the support and the enzyme after immobilization (Mohamad et al., 2015).

The accession number in UniProt database of the commercial L-ASNase from *E. coli* used in this work is P00805, meaning that it has about 348 amino acids and a mass of 139 kDa. The corresponding protein accession number was transferred to the ExPASy ProtParam tool, which estimated that the L-ASNase theoretical pI is around 5.66. However, this estimate may have some errors associated, due to L-ASNase quaternary structure and reported probable methylation, deamidation (Bae et al., 2011) and post translational modifications that are not accounted in the ProtParam model used.

Several authors reported an pI of L-ASNase of 4.9 (Liu et al. , 2013; Zhu et al., 2007), ranging between 4.6 to 5.1 accounting different mutations (Verma et al., 2014), which is somewhat different from the estimated theoretical pI.

Different approaches for the pI determination can be used. The simplest one, isoelectric precipitation, is based on the fact that the protein at pH values equal to pI has less solubility, thus consisting in varying the pH of a highly concentrated solution until protein precipitation. Obviously, this method has its drawbacks, since the protein can simply precipitate due to denaturation, for example. The most common procedures to determine protein pI are gel-based or capillary isoelectric focusing methods, where different molecules are separated by differences in their pI. In the gel-based isoelectric focusing method, a continuous pH gradient gel is created under the influence of an electric field, that will force the proteins to migrate to their pI. The capillary isoelectric focusing method uses a capillary column instead of the gel, achieving better resolution and sensitivity (Pihlasalo et al., 2012). Other less common methods used include chromatofocusing, discontinuous electrophoresis and ion-exchange chromatography (Pihlasalo et al., 2012).

In this work, the L-ASNase pI was determined using a method based on zeta potential, where the enzyme pI corresponds to the pH value where the zeta potential equals to zero (Salgin et al., 2012). The results are shown in Fig 10. Using the excel solver function to solve

the fourth-degree equation, it was found that the function intersects the zeta potential axis at pH 5.20. This means that the pI of the used L-ASNase is around 5.2, close to the values reported in the literature. The small differences can be explained by the use of different methods or by different ionic environments, such as ionic strength and ion type, that can cause changes in the enzyme pI (Salgin et al., 2012).

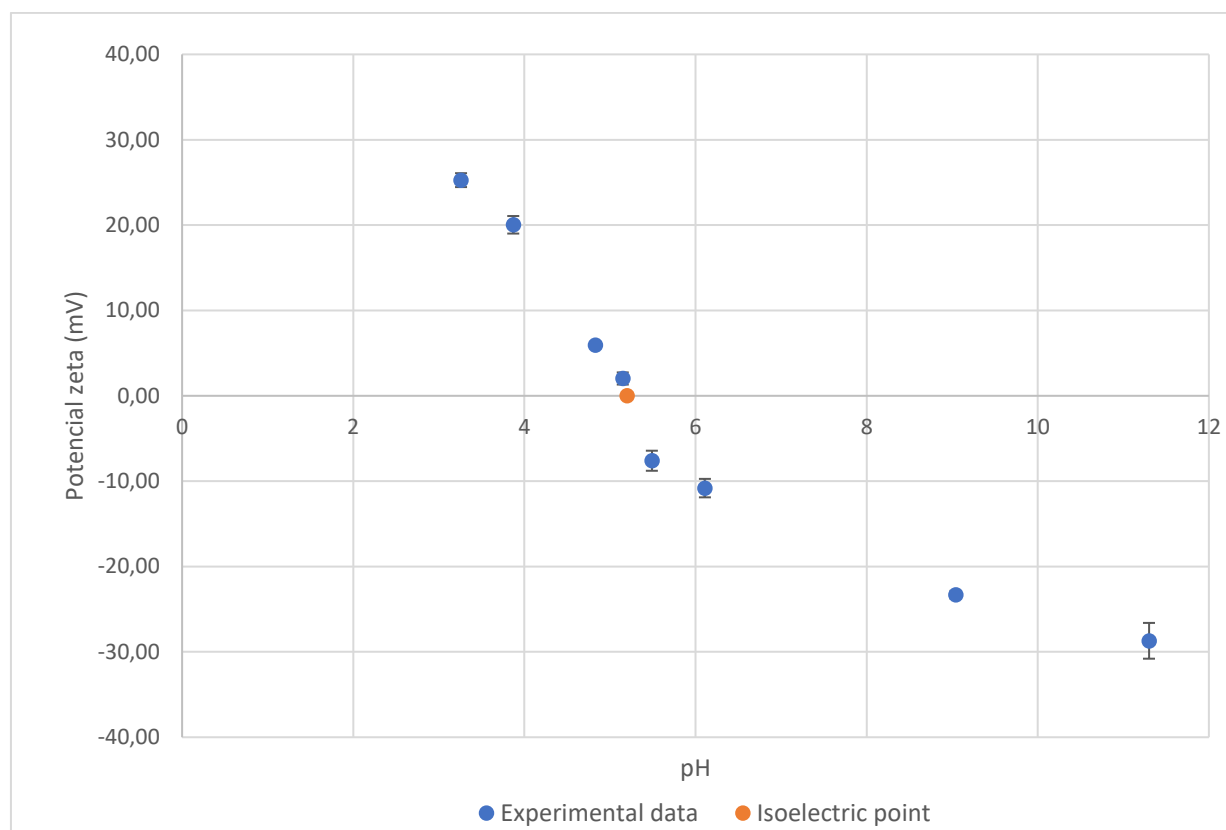


Figure 10 - L-ASNase potential zeta values for different pH values.

4.3 Effect of pH on L-ASNase onto CNTs

In this work, the immobilization of a commercial L-ASNase was studied through physical adsorption onto CNTs. The first parameter to be optimized was the pH of the immobilization medium. The enzyme immobilization onto a support is expected to be influenced by pH since it determines the protein and the CNTs superficial charges and, consequently, the affinity between them (Mohamad et al., 2015). However, it must be taken into account that, at certain pH values, the enzyme may exhibit low activity or even be denatured, therefore, the results can be inviable. This means that the pH study must have into account the pH ranges where the enzyme is more active. On the other hand, it is possible that the L-ASNase optimal pH will change after immobilization (Youssef & Al-Omar, 2008).

This way, the immobilization of 0.086 mg/mL of L-ASNase onto 2 mg of both pristine and carboxylic functionalized CNTs during 60 min was tested at different pH values (4, 6, 8 and 9). The L-ASNase activity was determined using the Nessler method. This colorimetric method determines the ammonium concentration released after the conversion of L-Asn into L-Asp and ammonia. The reaction between the produced ammonia and the Nessler reagent leads to the appearance of a yellow-brown precipitate. The colour will be more intense the greater the

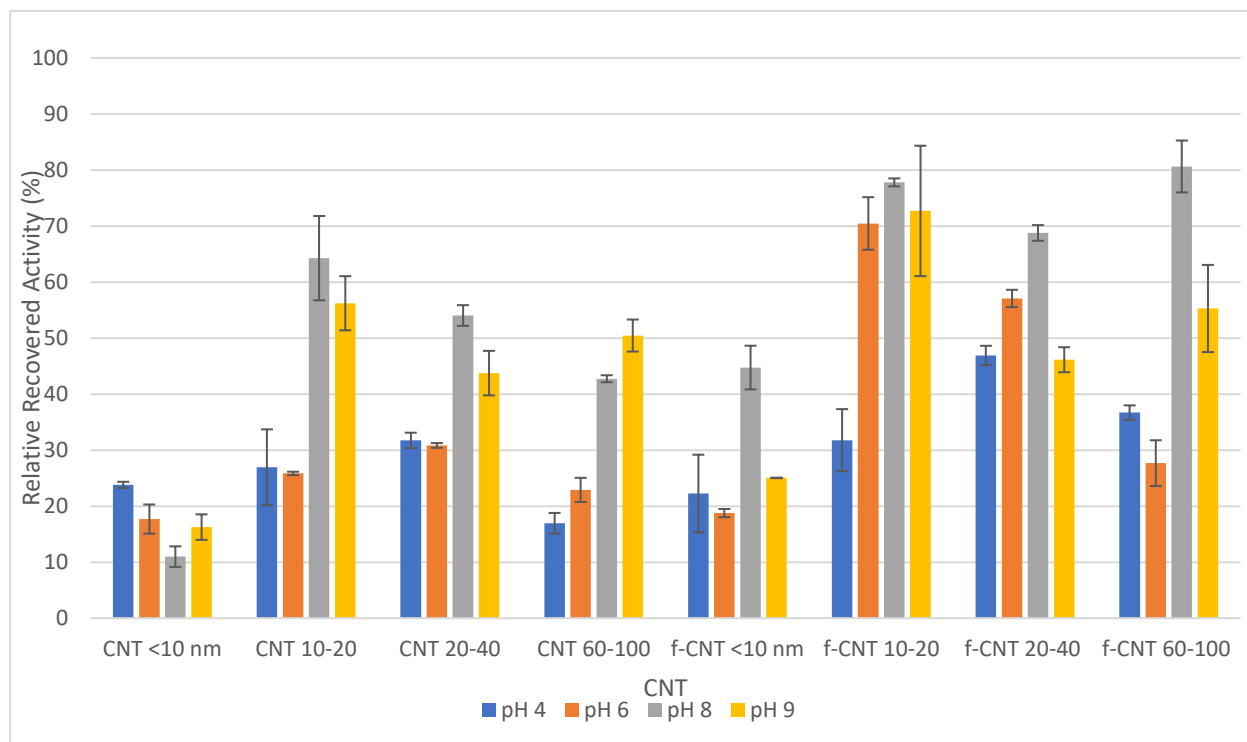


Figure 11 - Effect of pH on the relative recovered activity in the immobilization of 0.086 mg/mL of L-ASNase onto 2 mg of CNTs for 60 min of contact time.

concentration of the analysed substances. The NH_4^+ concentration is determined by absorption spectroscopy at $\lambda = 436$ nm. The calculated calibration curve is displayed on appendix 1. A control experiment with CNTs and Nessler reagent was also performed and no reaction or interference was detected. According to Fig 11, the highest RRA of immobilized L-ASNase occurred at pH 8 for almost all the CNTs tested, with the exception of the non-functionalized CNTs <10 nm and 60-100 nm CNTs, where the highest RRA were achieved at pH 4 and 9, respectively. In the case of f-CNT 10-20, the standard deviation was quite high, making unclear which pH showed the best results. In general, the highest RRA were attained at basic pH values. It is also possible to verify that the L-ASNase immobilized onto f-CNTs showed higher RRA than when immobilized onto pristine CNTs with the same diameters. This can be explained by the larger specific surface areas available to the L-ASNase adsorption and less hydrophobicity, that can increase enzyme biocompatibility.

Considering that the pI of L-ASNase is 5.2 and the PZC of pristine and functionalized CNTs is around 7 and 3, respectively, at pH 8, where the highest RRA were obtained, both enzyme and support surfaces are negatively charged, thus, electrostatic interactions are not likely to be the main driving force for the immobilization of L-ASNase under the used conditions. π - π interactions, CH- π interactions and hydrophobic interactions can be the cause of adsorption between CNTs and L-ASNase (Zhou et al., 2019).

The CNTs that displayed the best RRA (around 80%) were the f-CNT 10-20, revealing that they have the most adequate diameter and specific surface area in order to maintain the L-ASNase activity after immobilization as much as possible. Although <10 nm CNTs have a higher specific surface area, their diameter seems to be too small to keep all the enzymes molecules active. This means that the surface area of the CNTs is an important parameter during the L-ASNase immobilization, but the CNTs need to be of sufficient diameter so that the adsorbed enzymes have their active sites available to react with the substrate. Strikingly, f-CNT 60-100 had high RRA, although its specific area are one of the lowest.

Free L-ASNase activity was also examined at the studied pH values (Table 5), noting that fresh enzyme solutions were prepared in all experiments. No relevant shift in the pH where maximum activity is achieved was noted from free to immobilized enzyme during this experiment.

Table 5 - Activity of free L-ASNase (0.086 mg/mL) at different pH values.

Variable Condition	Free enzyme activity (U/mL)
pH 4	1.67
pH 6	4.26
pH 8	4.03
pH 9	2.23

The data in Table 5 show that free L-ASNase presents higher activities at pH values between 6 and 8, decreasing practically by half when it changes from pH 8 to 9. Comparing these results with the high relative recovered activities attained at pH 9 with the immobilized L-ASNase, it can be confirmed that the immobilization on CNTs made the L-ASNase more stable at basic pH values.

However, the efficacy of the immobilization should be analysed through a balance between the enzyme relative recovered activity and the immobilization yield results. The immobilization yields attained for the different pH values evaluated are presented in the Fig 12.

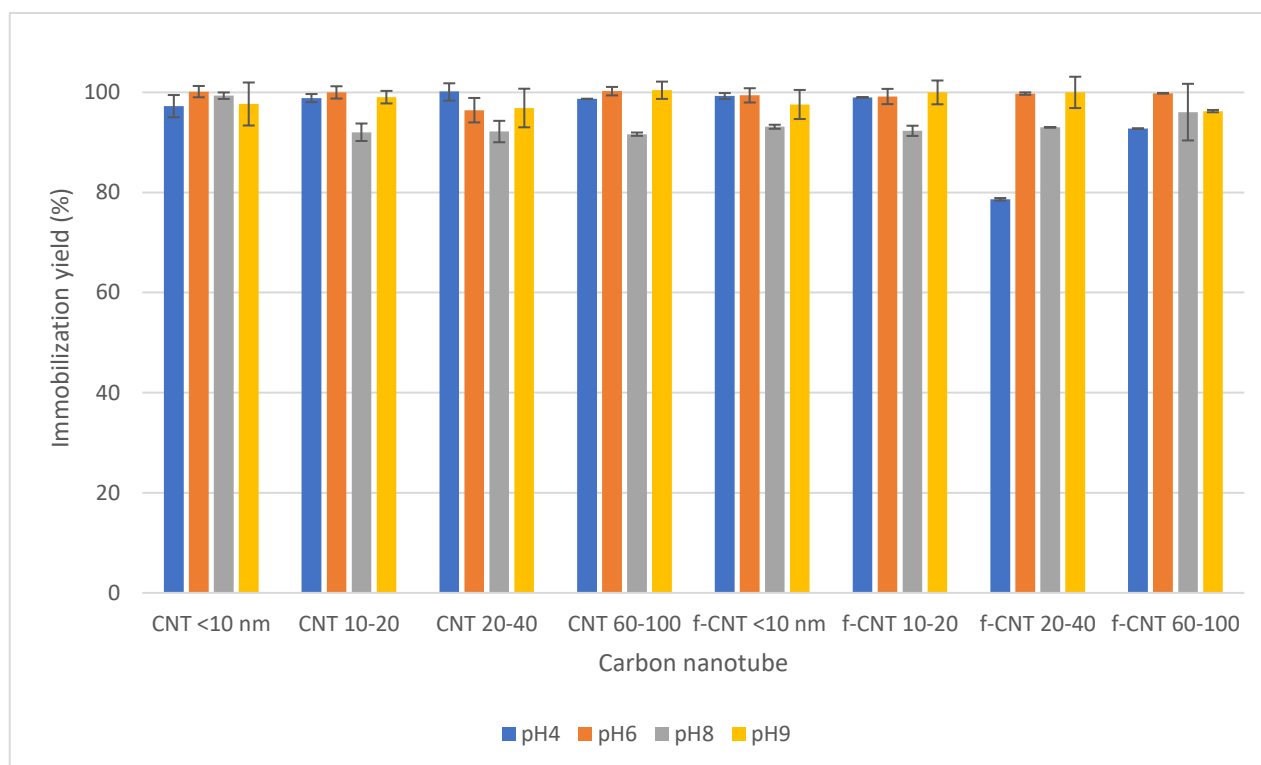


Figure 12 - Effect of pH on the immobilization yield (%) of L-ASNase (0.086 mg/mL) immobilization onto 2 mg of CNTs for 60 min of contact time.

According to Fig 12, it is possible to verify that in almost all the studied conditions immobilization yields above 90% were obtained, meaning almost total L-ASNase adsorption on CNTs. The f-CNT 20-40 were the exception, with an immobilization yield of only 79%, where a possible contamination of the supernatant with the CNTs occurred. The immobilization yield (IY) is calculated based on a relation between the free L-ASNase activity before immobilization and the activity of the free L-ASNase remaining in the supernatant after the immobilization. Therefore, taking into account that the higher values of IY are related to low supernatant L-ASNase activities and that these values are close to the absorbances of the blank samples, it should be noted that the accuracy of this method is lower for IY values closer to 100%.

The immobilization of L-ASNase on CNTs was already reported in literature. Haroun et al., (2020) studied -COOH functionalized CNTs as a support for an *Aspergillus versicolor* L-ASNase and reported higher YI values using a physical adsorption technique than with the covalent binding of the enzyme to the support, with a maximum YI attained of 54.4%. On the other hand, the immobilized L-ASNase retained 100% of the free enzyme activity.

The immobilization of L-ASNase has been also reported on other different supports, for example, Bahreini et al., (2014) described an immobilized L-ASNase on chitosan-tripolyphosphate nanoparticles with an entrapment efficiency around 72%. Agrawal et al. (2018) showed a maximum immobilization yield of 85% after optimizing the covalent L-ASNase immobilization on aluminium oxide pellets using response surface methodology and Golestaneh & Varshosaz, (2017) achieved an enzyme immobilization efficiency up to 95% on silica nanoparticles using 1-ethyl-3-(3-dimethylaminopropyl) carbodiimide HCl (EDC) and glutaraldehyde as cross-linkers. These results prove the potential of using CNTs as supports for the L-ASNase immobilization, reaching higher immobilizations yields (higher than 90%).

4.4 Effect of immobilization time on L-ASNase immobilization onto CNTs

To attain the maximum immobilization yield and relative recovered activity values the influence of immobilization contact time was also assessed. For that, the adsorption of 0.086 mg/mL of L-ASNase onto 2 mg of CNTs was evaluated for three different contact times (30, 60 and 120 min) at pH 8 (optimal immobilization pH). Higher immobilization times were expected to lead to higher RRA. The results of the effect of the immobilization time on the RRA are displayed in Fig 13, where it is possible to observe that when using pristine CNTs as immobilization support the RRA values increase till an immobilization time of 60 min for all the CNTs studied, with the exception of CNT< 10, where the best RRA was found for a contact time of 30 min. For higher contact times, probably a multi-layer of adsorbed L-ASNase (J. Wang et al., 2006) or an uncontrolled enzyme packing occurs, blocking the access of the substrate molecules to the active sites of L-ASNase, decreasing the RRA attained. It is worth noticing that for all cases, the RRA increased after CNTs functionalization, indicating the importance of this step for the efficiency of the biocatalytic process.

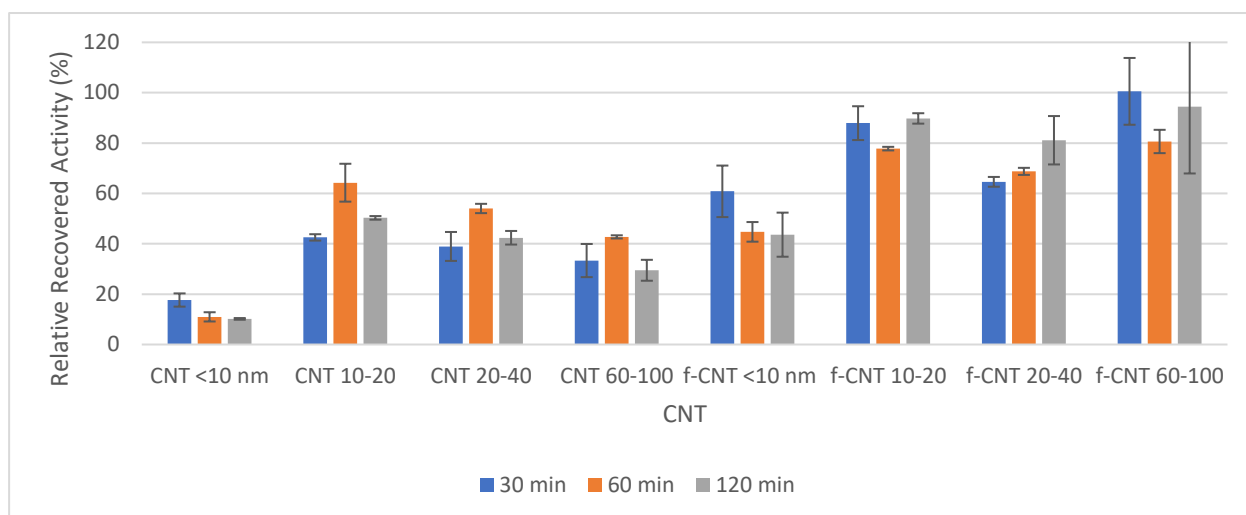


Figure 13 - Effect of immobilization time on the relative recovered activity in the immobilization of 0.086 mg/mL of L-ASNase onto 2 mg of CNTs at pH 8

The results presented in Fig 14 show that very high YI values (above 96%) are attained for all the studied samples with a contact time of only 30 min, reaching values of 100% after 120 min of immobilization time also practically for almost all the CNTs, meaning that the enzyme is totally adsorbed. These results corroborate the idea that a multi-layer enzyme adsorption must be occurring when using the pristine CNTs since, for a contact time of 120 min, the enzyme is totally adsorbed but with lesser RRA.

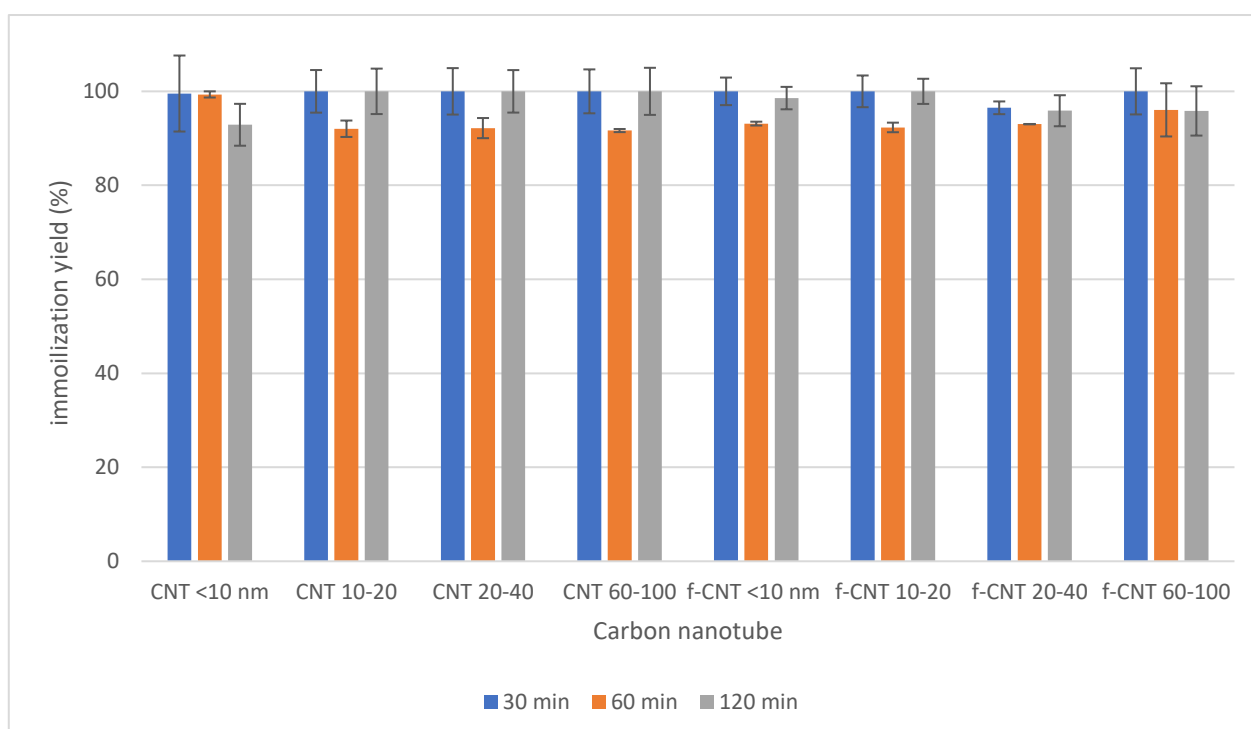


Figure 14 -Effect of immobilization time on the relative recovered activity in the immobilization of 0.086 mg/mL of L-ASNase onto 2 mg of CNTs at pH 8

One more time, the L-ASNase immobilization on f-CNTs showed better results in terms of RRA (Fig 14), probably due to the respective higher specific surface areas as was above mentioned. In the case of f-CNTs, considering the associated errors, it seems to have no difference between the results obtained for all the studied contact times, showing that it is not necessary to leave the enzyme in contact with the functionalized support for more than 30 min. It has to be noted, that, once more, the best results have been achieved with the f-CNT 10-20 and 60-100, with the last one reaching almost 100% RRA at the end of 30 min. However, as the standard deviation is too high, the sample must be redone. However, f-CNT 60-100 is one of the CNTs with lower surface area, meaning that apart from the surface area, other factors such as CNTs curvature and amount of surface groups may also play a role. A further study on these parameters is proposed as forthcoming work.

Due to the high RRA and IY yields attained it seems that, in general, the enzyme-to-CNT mass ratio used is close to the maximum enzyme adsorption capacity of most of the functionalized CNTs used, however this ratio must be optimized in future assays.

5 Conclusions

The main goal of this thesis was to optimize L-ASNase immobilization on CNTs. Considering the conditions tested, pH and immobilization time, the best overall results were obtained using functionalized CNTs, which may be mainly attributed to their higher specific surface areas comparing with the pristine materials. At pH 8, where free enzyme exhibited the highest activity, immobilized L-ASNase also showed the best relative recovered activities, achieving $80 \pm 8\%$ with f-CNT 60-100 and $78 \pm 12\%$ with f-CNT 10-20. The study of the pH effect on L-ASNase immobilization on CNTs showed an improvement in the L-ASNase stability at highly basic pH values when compared to the free enzyme.

The optimization of the immobilization time, carried out at pH 8, revealed higher RRA when using the functionalized CNTs, with f-CNT 60-100 achieving about 100% after 30 minutes of contact with L-ASNase. Immobilization yield was consistently higher than 90%, with the exception of f-CNT 20-40 at pH 4, showing the almost total enzyme adsorption on the support at all the operating conditions studied. The high RRA and immobilization yields attained after 30 min of contact between the L-ASNase and the functionalized CNTs, revealed that no longer immobilizations times are required.

The CNTs characterization showed that the treatment with nitric acid increased their specific surface area due to the creation of defect sites and/or holes on the sidewalls of the tubes. However, the surface area did not show to be directly related to the relative enzyme recovered activity within the results achieved with functionalized CNTs.

The determination of the L-ASNase isoelectric point by a zeta potential technique displayed an enzyme pI of 5.2, meaning that at the optimized pH (pH 8) the enzyme was negatively charged. These results and the negative surface of the CNTs at pH 8 revealed that the forces involved in the enzyme adsorption onto CNTs were not electrostatic, being probably attributed to hydrophobic, hydrogen or π - π bonds.

The results of this work demonstrate the potential of f-CNTs as promising supports for L-ASNase immobilization, which may drive to improved enzyme application in several fields, namely in pharmaceutical, food and in biosensing industries.

6 Future work

This work achieved very interesting results regarding the L-ASNase immobilization onto CNTs, however, there are still aspects that deserve further investigation, namely:

- i) To complete the important immobilization parameters optimization, mainly the L-ASNase to CNT mass ratio;
- ii) To determine the adsorption equilibrium isotherms to confirm or not the formation of L-ASNase multi-layers on the CNTs surface;
- iii) The protein amount in the supernatants can be tested by another method to ensure that the immobilization yield has been correctly determined. This can be achieved using the Bradford protein assay method;
- iv) To analyse the thermal, operational and storage stabilities of the complex enzyme-CNTs;
- v) To determine the kinetic parameters of both free and immobilized enzyme. This would help to better understand the behaviour of immobilized L-ASNase;
- vi) To deepen the knowledge about the enzyme and the support adsorption through additional characterization methods, for example using scanning electronic microscopy, Raman spectroscopy and thermogravimetric analysis;
- vii) To determine if CNTs curvature and amount of surface groups also play a role in RRA and IY.
- viii) Predicting a biomedical application, free and immobilized enzyme resistance tests to proteolytic enzymes and in vitro toxicity tests could also be carried out;
- ix) Predicting a food application for acrylamide mitigation, the measurement of the acrylamide content in fried potatoes pre-treated with immobilized L-ASNase during several cycles could be done;
- x) Predicting a purification application, the f-CNTs could be used in a fermentation broth at the optimized conditions for L-ASNase purification.

7 Final appreciation

My personal goals for this thesis were to learn new techniques and deepen my knowledge about protein immobilization and downstream processes. I think that these goals were achieved, while I proved to myself that I was able to achieve my ambition of the last few years, to carry out and write a master's thesis. Although I considered that the work performed was not very extensive due to the current pandemic, I think that the results contributed significantly to my personal progress as well as for NanoPurAsp project.

8 Bibliography

- Agrawal, S., Sharma, I., Prajapati, B. P., Suryawanshi, R. K., & Kango, N. (2018). Catalytic characteristics and application of L-asparaginase immobilized on aluminum oxide pellets. *International Journal of Biological Macromolecules*, *114*, 504-511. <https://doi.org/10.1016/j.ijbiomac.2018.03.081>
- Aiswarya, R., & Baskar, G. (2018). Enzymatic mitigation of acrylamide in fried potato chips using asparaginase from *Aspergillus terreus*. *International Journal of Food Science & Technology*, *53*(2), 491-498. <https://doi.org/10.1111/ijfs.13608>
- Ashrafi, H., Amini, M., Mohammadi-Samani, S., Ghasemi, Y., Azadi, A., Tabandeh, M. R., Kamali-Sarvestani, E., Daneshamouz, S. (2013). Nanostructure L-asparaginase-fatty acid bioconjugate: synthesis, preformulation study and biological assessment. *International Journal of Biological Macromolecules*, *62*, 180-187. <https://doi.org/10.1016/j.ijbiomac.2013.08.028>
- Asselin, B. L., Whiting, J. C., Coppola, D. J., Rupp, I. P., Sallan, S. E., & Cohen, H. J. (1993). Comparative pharmacokinetic studies of three asparaginase preparations. *Journal of Clinical Oncology*, *11*(9), 1780-1786. <https://doi.org/10.1200/JCO.1993.11.9.1780>
- Bae, N., Pollak, A., & Lubec, G. (2011). Proteins from *Erwinia* asparaginase Erwinase® and *E. coli* asparaginase 2 MEDAC® for treatment of human leukemia, show a multitude of modifications for which the consequences are completely unclear. *Electrophoresis*, *32*(14), 1824-1828. <https://doi.org/10.1002/elps.201100117>
- Bahreini, E., Aghaiypour, K., Abbasalipourkabir, R., Mokarram, A. R., Goodarzi, M. T., & Saidijam, M. (2014). Preparation and nanoencapsulation of l-asparaginase II in chitosan-tripolyphosphate nanoparticles and in vitro release study. *Nanoscale Research Letters*, *9*(1), 1-13. <https://doi.org/10.1186/1556-276X-9-340>
- Barillet, S., Simon-Deckers, A., Herlin-Boime, N., Mayne-L'Hermite, M., Reynaud, C., Cassio, D., Gouget, B., Carrière, M. (2010). Toxicological consequences of TiO₂, SiC nanoparticles and multi-walled carbon nanotubes exposure in several mammalian cell types: An in vitro study. *Journal of Nanoparticle Research*, *12*(1), 61-73. <https://doi.org/10.1007/s11051-009-9694-y>
- Batool, T., Makky, E. A., Jalal, M., & Yusoff, M. M. (2016). A Comprehensive Review on l-Asparaginase and Its Applications. *Applied Biochemistry and Biotechnology*, *178*(5), 900-923. <https://doi.org/10.1007/s12010-015-1917-3>
- Beckner, M. E. (2011). Encyclopedia of Cancer. In M. Schwab (Ed.), *Encyclopedia of Cancer*. <https://doi.org/10.1007/978-3-642-16483-5>
- Belson, M., Kingsley, B., & Holmes, A. (2007). Risk factors for acute leukemia in children: A review. *Environmental Health Perspectives*, *115*(1), 138-145. <https://doi.org/10.1289/ehp.9023>
- Borek, D., Michalska, K., Brzezinski, K., Kisiel, A., Podkowinski, J., Bonthron, D. T., Krowarsch, D., Otlewski, J., Jaskolski, M. (2004). Expression, purification and catalytic activity of *Lupinus luteus* asparagine β-amidohydrolase and its *Escherichia coli* homolog. *European Journal of Biochemistry*, *271*(15), 3215-3226. <https://doi.org/10.1111/j.1432-1033.2004.04254.x>
- Bozzone, D. M. (2009). *Leukemia (The Biology of Cancer)*. Chelsea House Pub (Library).
- Browne, E. K., Moore, C., Sykes, A., Lu, Z., Jeha, S., & Mandrell, B. N. (2018). Clinical Characteristics of Intravenous PEG-Asparaginase Hypersensitivity Reactions in Patients

- Undergoing Treatment for Acute Lymphoblastic Leukemia. *Journal of Pediatric Oncology Nursing*, 35(2), 103-109. <https://doi.org/10.1177/1043454217741868>
- Brumano, L. P., da Silva, F. V. S., Costa-Silva, T. A., Apolinário, A. C., Santos, J. H. P. M., Kleingesinds, E. K., Monteiro, G., Rangel-Yagui, C. de O., Benyahia, B., Junior, A. P. (2019). Development of L-asparaginase biobetters: Current research status and review of the desirable quality profiles. *Frontiers in Bioengineering and Biotechnology*, 6(JAN), 1-22. <https://doi.org/10.3389/fbioe.2018.00212>
- Burke, M. J., & Rheingold, S. R. (2017, March 4). Differentiating hypersensitivity versus infusion-related reactions in pediatric patients receiving intravenous asparaginase therapy for acute lymphoblastic leukemia. *Leukemia and Lymphoma*, Vol. 58, pp. 540-551. <https://doi.org/10.1080/10428194.2016.1213826>
- Cachumba, J. J. M., Antunes, F. A. F., Peres, G. F. D., Brumano, L. P., Santos, J. C. Dos, & Da Silva, S. S. (2016). Current applications and different approaches for microbial L-asparaginase production. *Brazilian Journal of Microbiology*, 47, 77-85. <https://doi.org/10.1016/j.bjm.2016.10.004>
- Clark, D. S. (1994). Can immobilization be exploited to modify enzyme activity? *Trends in Biotechnology*, 12(11), 439-443. [https://doi.org/10.1016/0167-7799\(94\)90018-3](https://doi.org/10.1016/0167-7799(94)90018-3)
- Di Francesco, A., Mari, M., Ugolini, L., Parisi, B., Genovese, J., Lazzeri, L., & Baraldi, E. (2019). Reduction of acrylamide formation in fried potato chips by *Aureobasidium pullulans* L1 strain. *International Journal of Food Microbiology*, 289(June 2018), 168-173. <https://doi.org/10.1016/j.ijfoodmicro.2018.09.018>
- Dinndorf, P. A., Gootenberg, J., Cohen, M. H., Keegan, P., & Pazdur, R. (2007). FDA Drug Approval Summary: Pegaspargase (Oncaspar®) for the First-Line Treatment of Children with Acute Lymphoblastic Leukemia (ALL). *The Oncologist*, 12(8), 991-998. <https://doi.org/10.1634/theoncologist.12-8-991>
- Elnashar, M. M. M. (2010). Review Article: Immobilized Molecules Using Biomaterials and Nanobiotechnology. *Journal of Biomaterials and Nanobiotechnology*, 01(01), 61-77. <https://doi.org/10.4236/jbmb.2010.11008>
- Elnashar, M. M. M., & Hassan, M. E. (2014). Novel Epoxy Activated Hydrogels for Solving Lactose Intolerance. *BioMed Research International*, 2014(6), 1-9. <https://doi.org/10.1155/2014/817985>
- Ettinger, L. J., Ettinger, A. G., Avramis, V. I., & Gaynon, P. S. (1997). Acute lymphoblastic leukaemia. A guide to asparaginase and pegaspargase therapy. *BioDrugs*, 7(1), 30-39. <https://doi.org/10.2165/00063030-199707010-00005>
- Felman, A. (2019). What to know about leukemia. Retrieved May 25, 2020, from <https://www.medicalnewstoday.com/articles/142595>
- Feng, W., & Ji, P. (2011). Enzymes immobilized on carbon nanotubes. *Biotechnology Advances*, 29(6), 889-895. <https://doi.org/10.1016/j.biotechadv.2011.07.007>
- Fernandes, C. S. M., Teixeira, G. D. G., Iranzo, O., & Roque, A. C. A. (2018). Engineered Protein Variants for Bioconjugation. In *Biomedical Applications of Functionalized Nanomaterials* (pp. 105-138). <https://doi.org/10.1016/B978-0-323-50878-0.00005-7>
- First “Acrylamide-Free” Biscuits Will Be Launched in Germany. (2007). Retrieved May 5, 2020, from First “Acrylamide-Free” Biscuits Will Be Launched in Germany website: [/www.foodingredientsfirst.com](http://www.foodingredientsfirst.com)
- Friedman, M. (2015). Acrylamide: Inhibition of formation in processed food and mitigation of toxicity in cells, animals, and humans. *Food and Function*, 6(6), 1752-1772.

<https://doi.org/10.1039/c5fo00320b>

- Gao, Y., & Kyratzis, I. (2008). Covalent immobilization of proteins on carbon nanotubes using the cross-linker 1-ethyl-3-(3-dimethylaminopropyl)carbodiimide - A critical assessment. *Bioconjugate Chemistry*, 19(10), 1945-1950. <https://doi.org/10.1021/bc800051c>
- Ghasemian, A., Al-marzoqi, A., Al-abodi, H. R., Alghanimi, Y. K., Kadhum, S. A., Shokouhi Mostafavi, S. K., & Fattahi, A. (2019). Bacterial l -asparaginases for cancer therapy: Current knowledge and future perspectives. *Journal of Cellular Physiology*, 234(11), 19271-19279. <https://doi.org/10.1002/jcp.28563>
- Ghosh, S., Chaganti, S. R., & Prakasham, R. S. (2012). Polyaniline nanofiber as a novel immobilization matrix for the anti-leukemia enzyme l-asparaginase. *Journal of Molecular Catalysis B: Enzymatic*, 74(1-2), 132-137. <https://doi.org/10.1016/j.molcatb.2011.09.009>
- Global Cancer Observatory. (2019). Retrieved December 23, 2019, from International Agency for Research on Cancer website: <http://gco.iarc.fr/today/home>
- Golestaneh, D., & Varshosaz, J. (2017). Enhancement in Biological Activity of L-Asparaginase by its Conjugation on Silica Nanoparticles. *Recent Patents on Nanotechnology*, 12(1), 70-82. <https://doi.org/10.2174/0929867324666170823143634>
- Guo, J., Zhang, X., Li, Q., & Li, W. (2007). Biodistribution of functionalized multiwall carbon nanotubes in mice. *Nuclear Medicine and Biology*, 34(5), 579-583. <https://doi.org/10.1016/j.nucmedbio.2007.03.003>
- Gupta, M. N., Kaloti, M., Kapoor, M., & Solanki, K. (2011). Nanomaterials as matrices for enzyme immobilization. *Artificial Cells, Blood Substitutes, and Biotechnology*, 39(2), 98-109. <https://doi.org/10.3109/10731199.2010.516259>
- Haroun, A. A., & Ahmed, F. (2020). Production, characterization and immobilization of *Aspergillus versicolor* L-asparaginase onto multi-walled carbon nanotubes. *Biointerface Research in Applied Chemistry*, 10(4), 5733-5740. <https://doi.org/10.33263/briac104.733740>
- Hoelzer, D., Bassan, R., Dombret, H., Fielding, A., Ribera, J. M., Buske, C., & on behalf of the ESMO Guidelines Committee, clinicalguidelines@esmo.org. (2016). Acute lymphoblastic leukaemia in adult patients: ESMO clinical practice guidelines for diagnosis, treatment and follow-up. *Annals of Oncology*, 27, v69-v82. <https://doi.org/10.1093/annonc/mdw025>
- Homaei, A. A., Sariri, R., Vianello, F., & Stevanato, R. (2013). Enzyme immobilization: An update. *Journal of Chemical Biology*, 6(4), 185-205. <https://doi.org/10.1007/s12154-013-0102-9>
- Hou, J., Xu, L., Han, Y., Tang, Y., Wan, H., Xu, Z., & Zheng, S. (2019). Deactivation and regeneration of carbon nanotubes and nitrogen-doped carbon nanotubes in catalytic peroxymonosulfate activation for phenol degradation: variation of surface functionalities. *RSC Advances*, 9(2), 974-983. <https://doi.org/10.1039/C8RA07696K>
- Hu, C. Y., Xu, Y. J., Duo, S. W., Zhang, R. F., & Li, M. S. (2009). Non-covalent functionalization of carbon nanotubes with surfactants and polymers. *Journal of the Chinese Chemical Society*, 56(2), 234-239. <https://doi.org/10.1002/jccs.200900033>
- Iacobucci, I., & Mullighan, C. G. (2017, March 20). Genetic basis of acute lymphoblastic leukemia. *Journal of Clinical Oncology*, Vol. 35, pp. 975-983. <https://doi.org/10.1200/JCO.2016.70.7836>
- Izadpanah Qeshmi, F., Homaei, A., Fernandes, P., & Javadpour, S. (2018). Marine microbial L-

- asparaginase: Biochemistry, molecular approaches and applications in tumor therapy and in food industry. *Microbiological Research*, 208, 99-112.
<https://doi.org/10.1016/j.micres.2018.01.011>
- Jaskólski, M., Kozak, M., Lubkowski, J., Palm, G., & Wlodawer, A. (2001). Structures of two highly homologous bacterial L-asparaginases: A case of enantiomorphic space groups. *Acta Crystallographica Section D: Biological Crystallography*, 57(3), 369-377.
<https://doi.org/10.1107/S0907444900020175>
- Jennings, M. P., & Beacham, I. R. (1993). Co-dependent positive regulation of the ansB F promoter of *Escherichia coli* by CRP and the FNR protein: a molecular analysis. *Molecular Microbiology*, 9(1), 155-164. <https://doi.org/10.1111/j.1365-2958.1993.tb01677.x>
- Kamble, K. D., Bidwe, P. R., Muley, V. Y., Kamble, L. H., Bhadange, D. G., & Musaddiq, M. (2012). Characterization of L-Asparaginase producing bacteria from water, farm and saline soil. *Bioscience Discovery*, 3(1), 116-119.
- Kattimani, L., Amena, S., Nandareddy, V., & Mujugond, P. (2009). Immobilization of *Streptomyces gulbargensis* in Polyurethane Foam: A Promising Technique for L-asparaginase Production on. *Iranian Journal of Biotechnology*, 7(4), 199-204. Retrieved from http://www.ijbiotech.com/article_7085.html
- Kloos, R. Q. H., Uyl-de Groot, C. A., van Litsenburg, R. R. L., Kaspers, G. J. L., Pieters, R., & van der Sluis, I. M. (2017). A cost analysis of individualized asparaginase treatment in pediatric acute lymphoblastic leukemia. *Pediatric Blood & Cancer*, 64(12), e26651.
<https://doi.org/10.1002/pbc.26651>
- Kumar, N. S. M., Shimray, C. A., Indrani, D., & Manonmani, H. K. (2014). Reduction of Acrylamide Formation in Sweet Bread with L-Asparaginase Treatment. *Food and Bioprocess Technology*, 7(3), 741-748. <https://doi.org/10.1007/s11947-013-1108-6>
- Kumar, S., Rani, R., Dilbaghi, N., Tankeshwar, K., & Kim, K. H. (2017). Carbon nanotubes: A novel material for multifaceted applications in human healthcare. *Chemical Society Reviews*, 46(1), 158-196. <https://doi.org/10.1039/c6cs00517a>
- Li, J. G., Li, Q. N., Xu, J. Y., Cal, X. O., Liu, R. L., Li, Y. J., Ma, J. F., Li, W. X. (2009). The pulmonary toxicity of multi-wall carbon nanotubes in mice 30 and 60 days after inhalation exposure. *Journal of Nanoscience and Nanotechnology*, 9(2), 1384-1387.
<https://doi.org/10.1166/jnn.2009.C162>
- Li, R., Wang, X., Ji, Z., Sun, B., Zhang, H., Chang, C. H., ... Xia, T. (2013). Surface Charge and Cellular Processing of Covalently Functionalized Multiwall Carbon Nanotubes Determine Pulmonary Toxicity. *ACS Nano*, 7(3), 2352-2368. <https://doi.org/10.1021/nn305567s>
- Likodimos, V., Steriotis, T. A., Papageorgiou, S. K., Romanos, G. E., Marques, R. R. N., Rocha, R. P., Falaras, P. (2014). Controlled surface functionalization of multiwall carbon nanotubes by HNO₃ hydrothermal oxidation. *Carbon*, 69, 311-326.
<https://doi.org/10.1016/j.carbon.2013.12.030>
- Liu, A. (2012). In vivo studies of the toxicity of multi-wall carbon nanotubes. *Advanced Materials Research*, 345, 287-291.
<https://doi.org/10.4028/www.scientific.net/AMR.345.287>
- Liu, C., Luo, L., & Lin, Q. (2019). Antitumor activity and ability to prevent acrylamide formation in fried foods of asparaginase from soybean root nodules. *Journal of Food Biochemistry*, 43(3), e12756. <https://doi.org/10.1111/jfbc.12756>
- Liu, W., Wang, H., Wang, W., Zhu, M., Liu, C., Wang, J., & Lu, Y. (2016). Use of PEG-asparaginase in newly diagnosed adults with standard-risk acute lymphoblastic leukemia

- compared with *E. coli*-asparaginase: a retrospective single-center study. *Scientific Reports*, 6(1), 39463. <https://doi.org/10.1038/srep39463>
- Liu, Y., Pietzsch, M., & Ulrich, J. (2013). Purification of L-asparaginase II by crystallization. *Frontiers of Chemical Science and Engineering*, 7(1), 37-42. <https://doi.org/10.1007/s11705-013-1303-z>
- LN, R., Doble, M., Rekha, V. P. B., & Pulicherla, K. K. (2011). In silico Engineering of L-Asparaginase to Have Reduced Glutaminase Side Activity for Effective Treatment of Acute Lymphoblastic Leukemia. *Journal of Pediatric Hematology/Oncology*, 33(8), 617-621. <https://doi.org/10.1097/MPH.0b013e31822aa4ec>
- Lopes, A. M., Oliveira-Nascimento, L. de, Ribeiro, A., Tairum, C. A., Breyer, C. A., Oliveira, M. A. de, Pessoa, A. (2017). Therapeutic L-asparaginase: upstream, downstream and beyond. *Critical Reviews in Biotechnology*, 37(1), 82-99. <https://doi.org/10.3109/07388551.2015.1120705>
- Magri, A., Soler, M. F., Lopes, A. M., Cilli, E. M., Barber, P. S., Pessoa, A., & Pereira, J. F. B. (2018). A critical analysis of L-asparaginase activity quantification methods—colorimetric methods versus high-performance liquid chromatography. *Analytical and Bioanalytical Chemistry*, 410(27), 6985-6990. <https://doi.org/10.1007/s00216-018-1326-x>
- Marques, R. R. N., Machado, B. F., Faria, J. L., & Silva, A. M. T. (2010). Controlled generation of oxygen functionalities on the surface of Single-Walled Carbon Nanotubes by HNO₃ hydrothermal oxidation. *Carbon*, 48(5), 1515-1523. <https://doi.org/10.1016/j.carbon.2009.12.047>
- Min, Y., Sun, H., Moon, C., Yockman, J., Jeong, Y., Kwon, Y. M., Yang, V. C. (2009). L-Asparaginase encapsulated intact erythrocytes for treatment of acute lymphoblastic leukemia (ALL). *Journal of Controlled Release : Official Journal of the Controlled Release Society*, 139(3), 182-189. <https://doi.org/10.1016/j.jconrel.2009.06.027>
- Miranda-Filho, A., Piñeros, M., Ferlay, J., Soerjomataram, I., Monnereau, A., & Bray, F. (2018). Epidemiological patterns of leukaemia in 184 countries: a population-based study. *The Lancet Haematology*, 5(1), e14-e24. [https://doi.org/10.1016/S2352-3026\(17\)30232-6](https://doi.org/10.1016/S2352-3026(17)30232-6)
- Mohamad, N. R., Marzuki, N. H. C., Buang, N. A., Huyop, F., & Wahab, R. A. (2015). An overview of technologies for immobilization of enzymes and surface analysis techniques for immobilized enzymes. *Biotechnology & Biotechnological Equipment*, 29(2), 205-220. <https://doi.org/10.1080/13102818.2015.1008192>
- Mohammadi, Z. A., Aghamiri, S. F., Zarrabi, A., & Talaie, M. R. (2015). A comparative study on non-covalent functionalization of carbon nanotubes by chitosan and its derivatives for delivery of doxorubicin. *Chemical Physics Letters*, 642, 22-28. <https://doi.org/10.1016/j.cplett.2015.10.075>
- Moharam, M. E., Gamal-Eldeen, A. M., & El-Sayed, S. T. (2010). Production, Immobilization and Anti-tumor Activity of L- Asparaginase of *Bacillus* sp R36. *Journal of American Science*, 6(8), 157-165. Retrieved from <http://www.americanscience.org>
- Monteiro-Riviere, N. A., Nemanich, R. J., Inman, A. O., Wang, Y. Y., & Riviere, J. E. (2005). Multi-walled carbon nanotube interactions with human epidermal keratinocytes. *Toxicology Letters*, 155(3), 377-384. <https://doi.org/10.1016/j.toxlet.2004.11.004>
- Mubarak, N. M., Yusof, F., & Alkhatib, M. F. (2011). The production of carbon nanotubes using two-stage chemical vapor deposition and their potential use in protein purification. *Chemical Engineering Journal*, 168(1), 461-469. <https://doi.org/10.1016/j.cej.2011.01.045>

- Muslim, S. N., Kadmy, I. M. S. A. L., Hussein, N. H., Naseer, A., Ali, M., & Dwaish, A. S. (2015). Enhancement of the Activity and Stability of L-Asparaginase Food Additive Purified from *Acinetobacter Baumannii* as Anticarcinogenic in Processed Foods. *International Journal of Advances in Chemical Engineering and Biological Sciences*, 2(1), 35-39. <https://doi.org/10.15242/ijacebs.c0815019>
- Narang, A. (2009, September 1). Quantitative effect and regulatory function of cyclic adenosine 5'-phosphate in *Escherichia coli*. *Journal of Biosciences*, Vol. 34, pp. 445-463. <https://doi.org/10.1007/s12038-009-0051-1>
- Narta, U. K., Kanwar, S. S., & Azmi, W. (2007). Pharmacological and clinical evaluation of l-asparaginase in the treatment of leukemia. *Critical Reviews in Oncology/Hematology*, 61(3), 208-221. <https://doi.org/10.1016/J.CRITREVONC.2006.07.009>
- Nguyen, H. H., & Kim, M. (2017). An Overview of Techniques in Enzyme Immobilization. *Applied Science and Convergence Technology*, 26(6), 157-163. <https://doi.org/10.5757/asct.2017.26.6.157>
- Pandey, A., Negi, S., & Soccol, C. R. (2007). *Current developments in biotechnology and bioengineering: production, isolation and purification of industrial products* (1st ed.; A. Pandey, S. Negi, & C. R. Soccol, Eds.). John Fedor.
- PDB RCSB Homepage (2020) Retrieved May 5, 2020, from <https://www.rcsb.org/>
- Phase I Study of mPEG-R-Crisantaspase Given IV. (2015). Retrieved May 18, 2020, from <https://clinicaltrials.gov/ct2/show/NCT01551524>
- Piątkowska-Jakubas, B., Krawczyk-Kuliś, M., Giebel, S., Adamczyk-Cioch, M., Czyż, A., Lech-Marańda, E., Paluszewska, M., Pałynyczko, G., Piszcz, J., Hołowiecki, J. (2008). Use of L-asparaginase in acute lymphoblastic leukemia: recommendations of the Polish Adult Leukemia Group. *Polish Archives of Internal Medicine*, 118(11), 664-669. <https://doi.org/10.20452/pamw.518>
- Pieters, R., Hunger, S. P., Boos, J., Rizzari, C., Silverman, L., Baruchel, A., Goekbuget, N., Schrappe, M., Pui, C.-H. (2011). L-asparaginase treatment in acute lymphoblastic leukemia. *Cancer*, 117(2), 238-249. <https://doi.org/10.1002/cncr.25489>
- Pihlasalo, S., Auranen, L., Hänninen, P., & Härmä, H. (2012). Method for estimation of protein isoelectric point. *Analytical Chemistry*, 84(19), 8253-8258. <https://doi.org/10.1021/ac301569b>
- Poznansky, M. J., Shandling, M., Salkie, M. A., Elliott, J. F., & Lau, E. (1982). Advantages in the Use of L-Asparaginase-Albumin Polymer as an Antitumor Agent. *Cancer Research*, 42(3), 1020-1025.
- Pui, C.-H., Robison, L. L., & Look, T. (2008). Acute lymphoblastic leukaemia. *The Lancet*, 371, 1030-1043. Retrieved from www.thelancet.com
- Ramya, L. N., Doble, M., Rekha, V. P. B., & Pulicherla, K. K. (2012). l-Asparaginase as Potent Anti-leukemic Agent and Its Significance of Having Reduced Glutaminase Side Activity for Better treatment of Acute Lymphoblastic Leukaemia. *Applied Biochemistry and Biotechnology*, 167(8), 2144-2159. <https://doi.org/10.1007/s12010-012-9755-z>
- Riehemann, K., Schneider, S. W., Luger, T. A., Godin, B., Ferrari, M., & Fuchs, H. (2009). Nanomedicine-Challenge and Perspectives. *Angewandte Chemie International Edition*, 48(5), 872-897. <https://doi.org/10.1002/anie.200802585>
- Rivera-Utrilla, J., Bautista-Toledo, I., Ferro-García, M. A., & Moreno-Castilla, C. (2001). Activated carbon surface modifications by adsorption of bacteria and their effect on aqueous lead adsorption. *Journal of Chemical Technology and Biotechnology*, 76(12),

- 1209-1215. <https://doi.org/10.1002/jctb.506>
- Saifuddin, N., Raziah, A. Z., & Junizah, A. R. (2013). Carbon nanotubes: A review on structure and their interaction with proteins. *Journal of Chemistry*, 2013, 18. <https://doi.org/10.1155/2013/676815>
- Salgin, S., Salgin, U., & Bahadir, S. (2012). Zeta potentials and isoelectric points of biomolecules: The effects of ion types and ionic strengths. *International Journal of Electrochemical Science*, 7(12), 12404-12414.
- Schipper, M. L., Nakayama-Ratchford, N., Davis, C. R., Kam, N. W. S., Chu, P., Liu, Z., Sun, X., Dai, H., Gambhir, S. S. (2008). A pilot toxicology study of single-walled carbon nanotubes in a small sample of mice. *Nature Nanotechnology*, 3(4), 216-221. <https://doi.org/10.1038/nnano.2008.68>
- Schmiegelow, K., Attarbaschi, A., Barzilai, S., Escherich, G., Frandsen, T. L., Halsey, C., ... Zapotocka, E. (2016). Consensus definitions of 14 severe acute toxic effects for childhood lymphoblastic leukaemia treatment: a Delphi consensus. *The Lancet Oncology*, 17(6), e231-e239. [https://doi.org/10.1016/S1470-2045\(16\)30035-3](https://doi.org/10.1016/S1470-2045(16)30035-3)
- Scientific Opinion on acrylamide in food. (2016). *EFSA Journal*, 13(6). <https://doi.org/10.2903/j.efsa.2015.4104>
- Scott, S., Busby, S., & Beacham, I. (1995). Transcriptional co-activation at the ansB promoters: Involvement of the activating regions of CRP and FNR when bound in tandem. *Molecular Microbiology*, 18(3), 521-531. https://doi.org/10.1111/j.1365-2958.1995.mmi_18030521.x
- Shakambari, G., Ashokkumar, B., & Varalakshmi, P. (2019). L-asparaginase - A promising biocatalyst for industrial and clinical applications. *Biocatalysis and Agricultural Biotechnology*, 17(October 2018), 213-224. <https://doi.org/10.1016/j.bcab.2018.11.018>
- Shim, M., Shi Kam, N. W., Chen, R. J., Li, Y., & Dai, H. (2002). Functionalization of Carbon Nanotubes for Biocompatibility and Biomolecular Recognition. *Nano Letters*, 2(4), 285-288. <https://doi.org/10.1021/nl015692j>
- Silva, C. G., Tavares, A. P. M., Dražić, G., Silva, A. M. T., Loureiro, J. M., & Faria, J. L. (2014). Controlling the surface chemistry of multiwalled carbon nanotubes for the production of highly efficient and stable laccase-based biocatalysts. *ChemPlusChem*, 79(8), 1116-1122. <https://doi.org/10.1002/cplu.201402054>
- Soares, A. L., Guimarães, G. M., Polakiewicz, B., Pitombo, R. N. D. M., & Abrahão-Neto, J. (2002). Effects of polyethylene glycol attachment on physicochemical and biological stability of *E. coli* L-asparaginase. *International Journal of Pharmaceutics*, 237(1-2), 163-170. [https://doi.org/10.1016/S0378-5173\(02\)00046-7](https://doi.org/10.1016/S0378-5173(02)00046-7)
- Srikhanta, Y. N., Atack, J. M., Beacham, I. R., & Jennings, M. P. (2013). Distinct physiological roles for the two l-asparaginase isozymes of *Escherichia coli*. *Biochemical and Biophysical Research Communications*, 436(3), 362-365. <https://doi.org/10.1016/j.bbrc.2013.05.066>
- Suma, Y., Kang, C. S., & Kim, H. S. (2016). Noncovalent and covalent immobilization of oxygenase on single-walled carbon nanotube for enzymatic decomposition of aromatic hydrocarbon intermediates. *Environmental Science and Pollution Research*, 23(2), 1015-1024. <https://doi.org/10.1007/s11356-015-4168-5>
- Surdyk, N., Rosén, J., Andersson, R., & Åman, P. (2004). Effects of Asparagine, Fructose, and Baking Conditions on Acrylamide Content in Yeast-Leavened Wheat Bread. *Journal of Agricultural and Food Chemistry*, 52(7), 2047-2051. <https://doi.org/10.1021/jf034999w>

- Swain, A. L., Jaskolski, M., Housset, D., Rao, J. K. M., & Wlodawer, A. (1993). Crystal structure of *Escherichia coli* L-asparaginase, an enzyme used in cancer therapy. *Proceedings of the National Academy of Sciences of the United States of America*, 90(4), 1474-1478. <https://doi.org/10.1073/pnas.90.4.1474>
- Tabandeh, M. R., & Aminlari, M. (2009). Synthesis, physicochemical and immunological properties of oxidized inulin-L-asparaginase bioconjugate. *Journal of Biotechnology*, 141(3-4), 189-195. <https://doi.org/10.1016/j.jbiotec.2009.03.020>
- Teodor, E., Litescu, S.-C., Lazar, V., & Somoghi, R. (2009). Hydrogel-magnetic nanoparticles with immobilized l-asparaginase for biomedical applications. *Journal of Materials Science: Materials in Medicine*, 20(6), 1307-1314. <https://doi.org/10.1007/s10856-008-3684-y>
- Terwilliger, T., & Abdul-Hay, M. (2017). Acute lymphoblastic leukemia: a comprehensive review and 2017 update. *Blood Cancer Journal*, 7(6), e577. <https://doi.org/10.1038/bcj.2017.53>
- Tran, D. N., & Balkus, K. J. (2011). Perspective of Recent Progress in Immobilization of Enzymes. *ACS Catalysis*, 1(8), 956-968. <https://doi.org/10.1021/cs200124a>
- Ulu, A., & Ates, B. (2017). Immobilization of L -Asparaginase on Carrier Materials: A Comprehensive Review. *Bioconjugate Chemistry*, 28(6), 1598-1610. <https://doi.org/10.1021/acs.bioconjchem.7b00217>
- Ulu, A., Karaman, M., Yapıcı, F., Naz, M., Sayın, S., Saygılı, E. İ., & Ateş, B. (2020). The Carboxylated Multi-walled Carbon Nanotubes/l-Asparaginase Doped Calcium-Alginate Beads: Structural and Biocatalytic Characterization. *Catalysis Letters*, 150(6), 1679-1691. <https://doi.org/10.1007/s10562-019-03069-y>
- Van Tol, H. H. M., & Iijima, S. (1991). Helical microtubules of graphitic carbon. *Nature*, 354(6348), 56-58. <https://doi.org/10.1038/354056a0>
- Verma, S., Mehta, R. K., Maiti, P., Röhm, K. H., & Sonawane, A. (2014). Improvement of stability and enzymatic activity by site-directed mutagenesis of *E. coli* asparaginase II. *Biochimica et Biophysica Acta - Proteins and Proteomics*, 1844(7), 1219-1230. <https://doi.org/10.1016/j.bbapap.2014.03.013>
- Vidya, J., Sajitha, S., Ushasree, M. V., Sindhu, R., Binod, P., Madhavan, A., & Pandey, A. (2017). Genetic and metabolic engineering approaches for the production and delivery of L-asparaginases: An overview. *Bioresource Technology*, 245, 1775-1781. <https://doi.org/10.1016/j.biortech.2017.05.057>
- Vimal, A., & Kumar, A. (2017). Biotechnological production and practical application of L-asparaginase enzyme. *Biotechnology and Genetic Engineering Reviews*, 33(1), 40-61. <https://doi.org/10.1080/02648725.2017.1357294>
- Wacker, P., Land, V. J., Camitta, B. M., Kurtzberg, J., Pullen, J., Harris, J. M. B., & Shuster, J. J. (2007). Allergic Reactions to *E. coli* L -Asparaginase Do Not Affect Outcome in Childhood B-precursor Acute Lymphoblastic Leukemia - A Children's Oncology Group Study. *J Pediatr Hematol Oncol*, 29(9), 627-632.
- Walkey, C. D., & Chan, W. C. W. (2012). Understanding and controlling the interaction of nanomaterials with proteins in a physiological environment. *Chemical Society Reviews*, 41(7), 2780-2799. <https://doi.org/10.1039/c1cs15233e>
- Wang, J., Liu, G., & Lin, Y. (2006). Amperometric choline biosensor fabricated through electrostatic assembly of bienzyme/polyelectrolyte hybrid layers on carbon nanotubes. *Analyst*, 131(4), 477-483. <https://doi.org/10.1039/b516038c>

- Wang, L., Wei, L., Chen, Y., & Jiang, R. (2010). Specific and reversible immobilization of NADH oxidase on functionalized carbon nanotubes. *Journal of Biotechnology*, 150(1), 57-63. <https://doi.org/10.1016/j.jbiotec.2010.07.005>
- Warangkar, S. C., & Khobragade, C. N. (2009). Screening, enrichment and media optimization for L-asparaginase production. *Journal of Cell and Tissue Research*, 9(3), 1963-1968.
- Wolf, M., Wirth, M., Pittner, F., & Gabor, F. (2003). Stabilisation and determination of the biological activity of L-asparaginase in poly(D,L-lactide-co-glycolide) nanospheres. *International Journal of Pharmaceutics*, 256(1-2), 141-152. [https://doi.org/10.1016/s0378-5173\(03\)00071-1](https://doi.org/10.1016/s0378-5173(03)00071-1)
- Xu, F., Oruna-Concha, M.-J., & Elmore, J. S. (2016). The use of asparaginase to reduce acrylamide levels in cooked food. *Food Chemistry*, 210, 163-171. <https://doi.org/10.1016/j.foodchem.2016.04.105>
- Xu, R., Tang, R., Zhou, Q., Li, F., & Zhang, B. (2015). Enhancement of catalytic activity of immobilized laccase for diclofenac biodegradation by carbon nanotubes. *Chemical Engineering Journal*, 262, 88-95. <https://doi.org/10.1016/j.cej.2014.09.072>
- Youssef, M. M., & Al-Omair, M. A. (2008). Cloning, purification, characterization and immobilization of L-asparaginase II from *E. coli* W3110. *Asian Journal of Biochemistry*, Vol. 3, pp. 337-350. <https://doi.org/10.3923/ajb.2008.337.350>
- Yun, M. K., Nourse, A., White, S. W., Rock, C. O., & Heath, R. J. (2007). Crystal Structure and Allosteric Regulation of the Cytoplasmic *Escherichia coli* l-Asparaginase I. *Journal of Molecular Biology*, 369(3), 794-811. <https://doi.org/10.1016/j.jmb.2007.03.061>
- Zdarta, J., Meyer, A. S., Jesionowski, T., & Pinelo, M. (2018). A general overview of support materials for enzyme immobilization: Characteristics, properties, practical utility. *Catalysts*, 8(2). <https://doi.org/10.3390/catal8020092>
- Zhang, B., Dong, L.-W., Tan, Y.-X., Zhang, J., Pan, Y.-F., Yang, C., ... Wang, H.-Y. (2013). Asparagine synthetase is an independent predictor of surgical survival and a potential therapeutic target in hepatocellular carcinoma. *British Journal of Cancer*, 109(1), 14-23. <https://doi.org/10.1038/bjc.2013.293>
- Zhao, H. Y., Zheng, W., Meng, Z. X., Zhou, H. M., Xu, X. X., Li, Z., & Zheng, Y. F. (2009). Bioelectrochemistry of hemoglobin immobilized on a sodium alginate-multiwall carbon nanotubes composite film. *Biosensors and Bioelectronics*, 24(8), 2352-2357. <https://doi.org/10.1016/j.bios.2008.12.004>
- Zhou, Y., Fang, Y., & Ramasamy, R. (2019). Non-Covalent Functionalization of Carbon Nanotubes for Electrochemical Biosensor Development. *Sensors*, 19(2), 392. <https://doi.org/10.3390/s19020392>
- Zhu, J.-H., Yan, X.-L., Chen, H.-J., & Wang, Z.-H. (2007). In situ extraction of intracellular l-asparaginase using thermoseparating aqueous two-phase systems. *Journal of Chromatography A*, 1147(1), 127-134. <https://doi.org/10.1016/j.chroma.2007.02.035>

Appendix 1 - Calibration curve for ammonia quantification

The determination of a calibration curve is fundamental to relate absorbance to ammonia concentration. The calibration curve was prepared through reaction of multiple dilutions of an ammonium sulphate prepared stock solution (8.5 mg/mL) with Nessler reagent. In a first attempt, the prepared solutions were excessively concentrated, leading to the formation of a dark precipitate (Fig A1, falcon S1), thus the calibration curve was then determined using more diluted solutions (Fig A1, falcons B to D). With the results of this initial test, it was possible to estimate which concentrations of ammonia would correspond to absorbances close to 0 and 1 and to prepare several solutions with intermediate ammonium sulphate concentrations (Table A1) in order to obtain a suitable calibration curve.

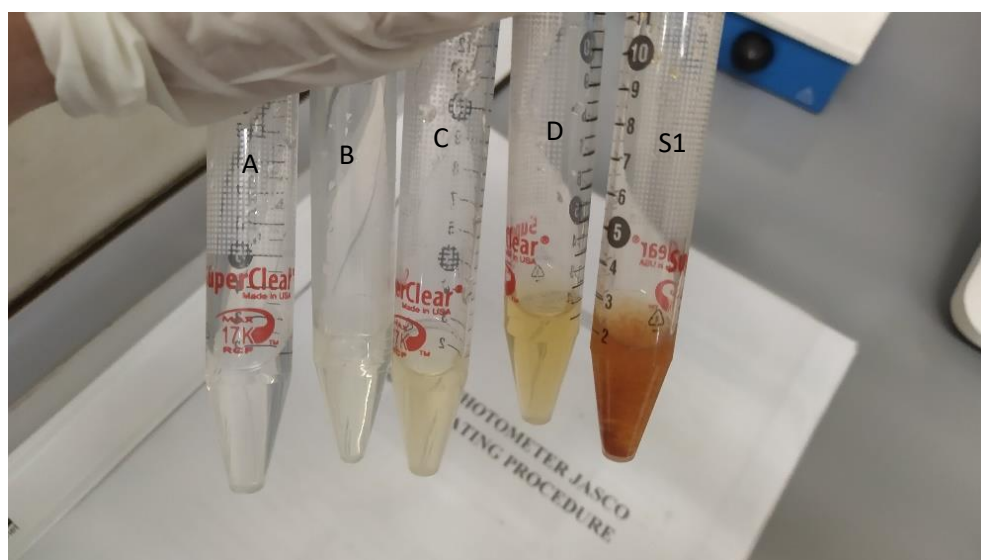


Figure A1 - Different ammonium sulphate dilutions after reaction with Nessler reagent: A - Blank, B - diluted 100x, C - diluted 25x, D - diluted 10x, S1 - stock solution.

The obtained calibration curve 1 (absorbance at 436 nm vs ammonium concentration) from the solutions prepared in table A1 is represented in Fig A2. The curve exhibits a R^2 of 0.9984, showing the good linearity in all the range of $ABS_{436\text{ nm}}$ tested. The detection and quantification limits were also calculated, in order to know the method limitations.

Table A1 - Ammonium standard solutions used to determine the calibration curve

Standard Solution	Estimated $ABS_{436\text{ nm}}$	Added volume of SS (mL)	Added volume of water (mL)	Final ammonia Concentration (mg/mL)
P0	0.000	0.00	2.25	0.00
P1	0.100	0.20	2.05	0.68
P2	0.200	0.40	1.85	1.35
P3	0.300	0.60	1.65	2.03
P4	0.400	0.80	1.45	2.71
P5	0.500	1.00	1.25	3.38
P6	0.600	1.20	1.05	4.06
P7	0.700	1.40	0.85	4.74
P8	0.800	1.70	0.55	5.75
P9	0.900	2.00	0.25	6.77
P10	1.000	2.25	0.00	7.61

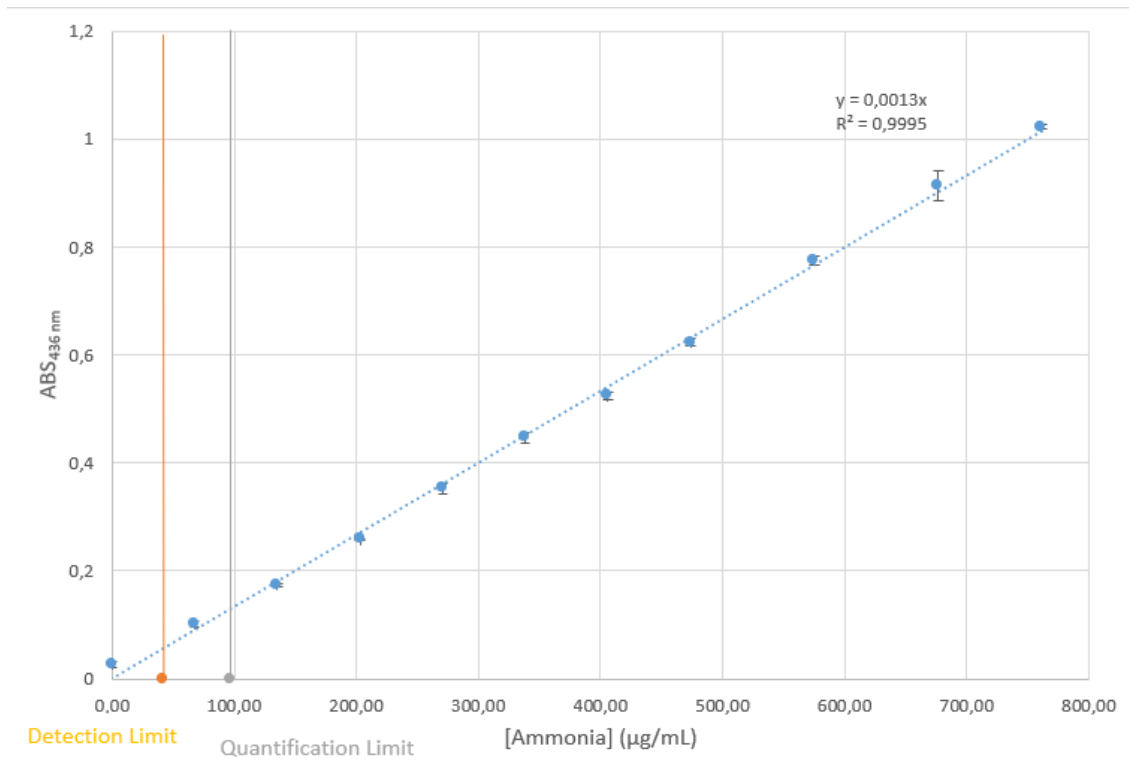


Figure A2 - Calibration curve for ammonium sulphate quantification.